

**University of Alberta**

**Single Chain Fraction Variable Binding Molecules as Bone-Targeting Therapeutics and  
Diagnostics**

by

**Michael Ching Wai Lam**

A thesis submitted to the Faculty of Graduate Studies and Research  
in partial fulfillment of the requirements for the degree of

**Master of Science**  
in  
**Pharmaceutical Sciences**

Pharmacy and Pharmaceutical Sciences

©Michael Ching Wai Lam  
Fall 2011  
Edmonton, Alberta

Permission is hereby granted to the University of Alberta Libraries to reproduce single copies of this thesis and to lend or sell such copies for private, scholarly or scientific research purposes only. Where the thesis is converted to, or otherwise made available in digital form, the University of Alberta will advise potential users of the thesis of these terms.

The author reserves all other publication and other rights in association with the copyright in the thesis and, except as herein before provided, neither the thesis nor any substantial portion thereof may be printed or otherwise reproduced in any material form whatsoever without the author's prior written permission.

## **Abstract**

Osteoporosis is a disease characterized by lowering of bone mass and subsequent bone fracture. Although successful antiresorptive treatment options are commercially available, they have disadvantages such as poor bioavailability and significant side effects. Using phage display, an in vitro high throughput screening method, we sought to generate single chain fraction variable (scFv) against osteoclast surface receptors and bone turnover markers, for the evaluation of their potential as drug-targeted delivery platforms for improved bioavailability of current therapeutics and as immunodiagnostic assay reagents in osteoporosis. With our current in vitro result, it can be concluded that scFv, although having weaker binding affinity than IgG antibody, still possesses good selective binding against antigens. With this method of generating scFv being more cost-effective and less labour intensive, scFv reagents can become a viable option in site-directed drug delivery and immunodiagnostic for osteoporosis and possibly for cross application to other bone-modifying disease such as osteoarthritis.

## **Acknowledgement**

First and foremost, I would like to thank Dr. Doschak for his supervision throughout this program. His guidance has been important for my success in this degree.

I would like to especially thank Biwen Xu for her continuous training and valuable advice over the course of my degree, particularly in providing her precious experience in many molecular biology techniques. Thank you to all other current lab members - Krishna Bhandari, Neel Kaipatur, Madhuri Newa, Arash Panahifar and Yuchin Wu – for the support throughout this degree. Thank you to all lab members of Dr. Suresh’s lab for their assistance.

I am also very grateful of my supervisory committee members – Dr. Suresh and Dr. Kaur – for their support and guidance.

# Table of Content

1.1. Osteoporosis: Overview .....	1
1.2. RANK/RANKL/OPG in Osteoclastogenesis and Their Potential as Antiresorptive Therapy Target.....	7
1.3. Current Treatment in Osteoporosis .....	14
1.3.1 Anabolic Agents.....	14
1.3.2 Antiresorptive Agents .....	16
1.4. Bone-turnover Markers .....	24
1.4.1. Bone Resorption Markers .....	24
1.4.2. Bone Formation Markers .....	27
1.4.3. Benefits and Limitations of Bone Turnover Markers in Diagnosis of Osteoporosis and other Bone-Modifying Diseases .....	29
1.5. Antibody Biologics and their Value as Therapeutics.....	29
1.5.1 Engineered Antibody Fragments.....	34
1.6. Phage Display .....	36
2. Overview and Hypothesis .....	45
3. Materials and Methods.....	49
3.1. Phage Display .....	49
3.1.1. Helper Phage Production .....	49
3.1.2. Amplification of Phage Library .....	51
3.1.3. Phage Production from Original Library .....	52
3.1.4. scFv Phage Selection .....	53
3.1.5. Phage Rescue and Propagation of Enriched scFv Phage .....	54
3.2. Post-Screening Analyses.....	55
3.2.1. Phage Enzyme-linked Immunosorbent Assay.....	55
3.2.2. DNA Sequencing .....	57
3.3. Production and Characterization of scFv .....	59
3.3.1. Infection of Positive scFv Phage Clone to <i>E.coli</i> HB2151 Expression Strain	59
3.3.2. Large Scale scFv Expression .....	60
3.3.3. Purification of Expressed scFv.....	61
3.3.4. Sodium Dodecylsulfate Polyacrylamide Gel Electrophoresis (SDS-PAGE)..	63
3.3.5. Western Blot .....	64

3.3.6. Enzyme-linked Immunosorbent Assay .....	65
3.4. Development of Immunoassay.....	66
3.4.1. Antigen-scFv Titration.....	66
3.4.2. Competitive Enzyme-linked Immunosorbent Assay.....	67
4. Results.....	69
4.1. Development of RANK-binding scFv .....	69
4.1.1. Screening of RANK-binding Phage.....	69
4.1.2. Purification and Characterization of RANK-binding scFv .....	69
4.1.3. Comparison with Commercial RANK Antibody .....	74
4.2. Development of Osteocalcin-binding scFv .....	75
4.2.1. Screening of Osteocalcin-binding Phage .....	75
4.2.2. Purification and Characterization of Osteocalcin-binding scFv.....	77
4.2.3. Development of Immunoassay Using Purified Osteocalcin-binding scFv .....	80
4.3. Development of CTX-binding scFv.....	85
4.3.1. Screening of CTX-binding Phage .....	85
5. Discussion.....	88
5.1. Phage Display and Generation of scFv .....	88
5.2. Phage Display of RANK-binding scFv.....	90
5.3. Phage Display of Osteocalcin-binding scFv .....	94
5.4. Immunoassay Development of Osteocalcin-binding scFv.....	95
5.5. Phage Display of CTX-binding scFv .....	97
6. Conclusion .....	101
7. Future Directions .....	103
8. Bibliography .....	105

## List of Figures

Figure 1.1 Phases in Bone Remodeling

Figure 1.2 Signaling Cascade Initiated by RANKL.

Figure 1.3 Chemical Structure of Endogenous Pyrophosphate and Bisphosphonates.

Figure 1.4 M13 Filamentous Phage and scFv-displaying Phage.

Figure 1.5 Overall Concept of Phage Display.

Figure 4.1: Panning Efficiency of Phage Panning Against RANK.

Figure 4.2 Histogram of Anti-RANK Phage ELISA Abs<sub>650nm</sub> Reading.

Figure 4.3 Amino Acid Sequence of RANK-binding scFv.

Figure 4.4 SDS-PAGE of Ni-NTA Column Purification of anti-RANK scFv.

Figure 4.5 SDS-PAGE and Western Blot Images of dialyzed purified scFv.

Figure 4.6 ELISA of Serial Diluted scFv.

Figure 4.7 Comparative ELISA of Purified scFv against Commercial and In-lab Generated Hybridoma.

Figure 4.8 Panning Efficiency of Phage Panning Against Osteocalcin

Figure 4.9 Histogram of anti-Osteocalcin Phage ELISA Abs<sub>650nm</sub> Reading.

Figure 4.10 Amino Acid Alignment for Osteocalcin-binding scFv's.

Figure 4.11 SDS-PAGE of Purified Dialyzed anti-Osteocalcin scFv's.

Figure 4.12 Western Blot of Anti-Osteocalcin scFv's.

Figure 4.13 Western Blot of OC2 D1.

Figure 4.14 Dot Blot of OC1 Against Osteocalcin.

Figure 4.15 3D Bar Graph of "Checker Board" ELISA Titration using OC1.

Figure 4.16 Standard Curve of Osteocalcin Competitive Assay Using OC1 scFv.

Figure 4.17 Quantitation of Serum Osteocalcin Using scFv vs Commercial Assay.

Figure 4.18 Relative Comparison of Serum Osteocalcin Using scFv vs Commercial Assay

Figure 4.19 Panning Efficiency of Phage Panning Against CTX.

Figure 4.20 Histogram of Anti-CTX Phage ELISA  $Ab_{650nm}$  Reading.

Figure 4.21 Amino Acid Sequence of CTX-binding scFv-phage Fusion.

## List of Abbreviations

AP	Alkaline Phosphatase	NTX	Collagen Type I Crosslinked N-Telopeptide
APS	Ammonium Persulfate	OPG	Osteoprotegrin
ATP	Adenosine Tri-Phosphate	OVX	Ovariectomize
BCA	Bicinchoninic Acid	PICP	Carboxy-terminal Propeptides of Type I Collagen
BMD	Bone Mineral Density	P1NP	Amino-terminal Propeptides of Type I Collagen
BSA	Bovine Serum Albumin	PBS	Phosphate Buffered Saline
cDNA	Complementary Deoxyribonucleic Acid	PCR	Polymerase Chain Reaction
CDR	Complementary Determining Region	PEG	Polyethylene Glycol
CTX	Collagen Type I Crosslinked C-Telopeptide	PPi	Inorganic Pyrophosphate
dAb	Domain Antibody	PTH	Parathyroid Hormone
DNA	Deoxyribose Nucleic Acid	PYD	Pyridinoline
DXA	Dual X-ray Absorptiometry	RANK	Receptor Activator for Nuclear Factor $\kappa$ B
DYD	Deoxy pyridinoline	RANKL	Receptor Activator for Nuclear Factor $\kappa$ B Ligand
ELISA	Enzyme-Linked Immunosorbent Assay	RPM	Revolution Per Minute
Fab	Fragment of Antigen Binding	scFv	Single Chain Variable Fraction
HPLC	High Performance Liquid Chromatography	SDS-PAGE	Sodium Dodecyl Sulfate Polyacrylamide Gel Electrophoresis
HRP	Horse Radish Peroxidase	SERM	Selective Estrogen Receptor Modulator
Ig	Immunoglobulin	TEMED	Tetramethylethylenediamine
IPTG	Isopropyl Thiogalactopyranoside	TMB	Trimethylbenzidine
M-CSF	Macrophage Colony-Stimulating Factor	TNF	Tumour Necrosis Factor
mRNA	Messenger Ribonucleic Acid	TRAF	Tumour Necrosis Factor Receptor Associated Factor
MWCO	Molecular Weight Cutoff	TRANCE	Tumour Necrosis Factor-Related Activation-Induced Cytokine

NFAT	Nuclear Factor of Activated T-cells	TRAP	Tartrate-Resistant Acid Phosphatase
Ni- NTA	Nickel-Nitrilotriacetic Acid	YT	Yeast Tryptone

# 1. Literature Review

## 1.1. Osteoporosis: Overview

Osteoporosis is a disease characterized by low bone mass and deterioration of bone tissue, which subsequently leads to bone fragility and fractures in weight bearing area such as hip, spine and wrist (1). Although individuals of any age can be diagnosed with osteoporosis, the probability significantly increases as age increases. In Canada, almost 2 million Canadians are living with osteoporosis. However, in individuals over the age of 50, 1 in 8 men and 1 in 4 women are diagnosed with osteoporosis (1). In Canada alone, 30000 hip fractures occur annually, with osteoporosis accounting for 70-90%. Moreover, in the population aged 60 and over, osteoporosis is the cause of over 80% of bone fractures (1). On a cost basis, the Canadian healthcare system spends approximately \$1.9 billion per year on the treatment of osteoporosis and related complications such as fractures (1).

For the diagnosis of osteoporosis, bone mineral density (BMD) has been used as the gold standard (2). To simplify the assessment further, BMD is classified into categories, or thresholds, based on the values obtained from dual X-ray absorptiometry (3). Since the distribution of bone mineral density is close to a Gaussian distribution regardless of the technique used, a threshold score, or T-score, is assigned based on the standard deviation of an individual's measurement compared to the population reference mean (3). For example, women with hip BMD greater than 1 standard deviation below the young adult female reference mean are assigned a T-score of  $>-1$  (3). According to the World Health

Organization and International Osteoporosis Foundation, a T-score of  $>-1$  is considered normal, a T-score of  $<-2.5$  is considered osteoporotic and a T-score within the 2 limits is considered osteopenic, or having a low bone mass (2, 3).

Bone mineral content and density can be measured by a number of methods – Single and dual X-ray absorptiometry (DXA), which show an accuracy of 90% for hip scans, provide a 2-D picture instead of a 3-D volumetric measurement; Computed tomography, which is an improvement over DXA and used mostly for spine and other appendicular skeleton, provides excellent 3-D representation of the bone mineral content at selected regions, but comes with disadvantages of high cost and high exposure to radiation; Quantitative ultrasound, which is generally used for providing structural organization and bone mass information at heel by measuring either ultrasound attenuation or velocity, is a non-ionizing technique that cannot be used to diagnose osteoporosis, but rather used to assess the fracture risk in elderly women (3). Historically, T-score is often used for diagnosing osteoporosis as well as being a predictor of bone fracture risk since numerous studies have successfully correlated low bone mineral density (T-score  $< -2.5$ ) to increased chance of bone fracture (2). However, there has been a paradigm shift recently advocating for a more comprehensive assessment of fracture risk that is not based entirely on T-score (2). As such, many clinical situations have now started to use algorithms that look at T-score, history of fracture, personal and family history of fracture, living habits such as alcohol and cigarette consumption, glucocorticoid use and low bodyweight. Combining all of these mentioned factors allows the prediction of a 10-year probability of hip and

other fractures (2). In addition, several serum and urine biochemical bone turnover markers have been identified and methods for their quantification have recently been developed. These biomarkers, which will be discussed in detail in section 1.4, provide a non-invasive and inexpensive method to evaluate bone resorption and formation (2). Although these markers have yet to be recognized in clinical settings and have yet to find their value in the diagnosis of osteoporosis, there are already studies which report the correlation between increased level of bone resorption markers and increased risk of fracture in elderly women (2). Therefore, bone turnover markers have the potential, in combination with BMD T-score and additional risk factors, for predicting fracture risk independent of bone mineral density, and for evaluating and monitoring therapy and studying the pathogenesis of osteoporosis (2).

To understand the pathogenesis of osteoporosis, it is necessary to first understand the bone remodeling process at a cellular level. The human skeleton consists of many specialized cells, mineralized and unmineralized connective tissue matrix, and spaces that include the bone marrow cavity and vascular canals (4). It is a highly specialized organ that undergoes constant regeneration (4). During growth and development, the skeleton is sculpted by a process called modeling (4). Once the skeletal system reaches maturity, it undergoes periodic replacement of old bone with new at the same location (4). This process is called bone remodeling and it is estimated that a human regenerates a complete new skeleton every 10 years by this process (4). The bone remodeling process is a continuous cycle of bone removal, or bone resorption, by osteoclasts and bone

formation by osteoblasts. These two processes, although having opposite function, do not function independently of each other and are tightly regulated by one other. All osteoblasts and osteoclasts belong to a temporary bone multicellular unit, or BMU (4-6). A BMU consists of the aforementioned osteoclasts and osteoblasts, a central vascular capillary, a nerve supply, and associated connective tissue (4). BMUs can be found on either surface of trabecular bone as irregular Howship's lacunae or in cortical bone as relatively uniform cylindrical Haversian systems (6). In a healthy human, approximately 3-4 million BMUs are initiated each year and approximately 1 million are operating at any given time. Each BMU has a lifespan of 6-9 months, although the lifespan of osteoclasts and osteoblasts is 2 weeks and 3 months respectively, therefore a BMU is constantly being supplied with newly functional osteoclasts and osteoblasts from their respective progenitor cells in bone marrow (4). A BMU functions by initiating at a certain location on the bone and move towards sites for repair or replacement. Despite moving as a unit, BMU constantly maintain an organized spatial and temporal relationship between all components (4).

The bone remodeling process consists of 4 phases: initiation/activation, resorption, reversal and formation (5, 6). During initiation, osteoclast-precursor cells interact with retracting lining cells that are derived from osteoblasts and usually cover all bone surfaces (5-7). Once these precursor cells settle on the exposed bone surface, they will respond to signals from various cytokines to fuse and form multinucleated osteoclasts (5). The cytokines involved in osteoclastogenesis will be discussed in the section below. Once the osteoclasts are

activated, the 2<sup>nd</sup> phase of bone remodeling begins where bone removal, or bone resorption, occurs at a predetermined location over a period of 1-2 weeks (5, 7). After bone resorption has ended, osteoclasts will disappear from the bone surface and be replaced by mononucleated cells that are responsible for summoning osteoblast-precursor cells. This is known as the reversal phase. In this phase, osteoblast-precursor cells attach to the resorbed bone surface, differentiate into mature osteoblasts and participate in bone formation, the last phase of bone remodeling (5-7). The bone formation phase is significantly longer than the previous 3 phases and it involves osteoblasts producing new organic matrix at the resorbed surface. This matrix, or osteoid, will be mineralized after 25-35 days (5). Once osteoblasts have completed bone formation on the entire surface, they will either become lining cells and be embedded into bone as osteocytes, or undergo apoptosis (6).

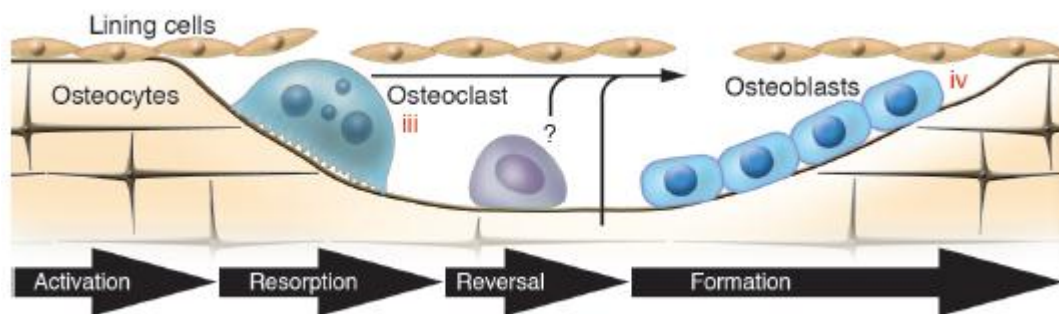


**Figure 6.1 Phases in Bone Remodeling.** Process proceeds from left to right. **i.** Activation – Lining cells retract, leaving bone expose for pre-osteoclast binding **ii.** Resorption – Mature osteoclasts undergo bone resorption at defined site **iii.** Reversal – osteoclasts disappear and pre-osteoblasts are recruited **iv.** Formation – Mature osteoblasts replenish resorbed surface with new material. Image taken from Raisz 2005 (6)

Since bone resorption and bone formation are tightly coupled processes that are kept under homeostasis under normal condition, a disruption to this

equilibrium will result in an imbalance. In the case of osteoporosis, this imbalance is a significant increase in bone resorption with no change or even a slight decrease in bone formation. This imbalance can be caused by a combination of age-related factors such as secondary hyperparathyroidism, reduced mechanical loading and estrogen deficiency in the case of postmenopausal women (2).

Estrogen is found to play a significant role in the normal bone remodeling process, such that its deficiency after menopause results in a dramatic increase in osteoclastogenesis and subsequent progressive loss of trabecular bone (2). Although it is widely accepted that osteoclast activity and osteoclastogenesis are regulated by the triad of receptor activator of nuclear factor  $\kappa$  B (RANK), its natural ligand (RANKL) and decoy receptor osteoprotegerin (OPG), estrogen is found to play an indirect role of regulating the release of these cytokines (2, 8). Before the signaling cascade between RANK, RANKL and OPG takes place, osteoclast progenitors are positively regulated by proinflammatory cytokines such as tumour necrosis factor and interleukin 1 (2). Furthermore, osteoclast apoptosis is also thought to be accelerated by the cytokine transforming growth factor  $\beta$  (2). Through studies of ovariectomized animals, an established osteoporosis model, it is found that estrogen negatively regulates tumour necrosis factor and interleukin 1 while increasing the production of transforming growth factor  $\beta$  (2). As a result, estrogen deficiency disrupts the bone remodeling imbalance indirectly by significantly increasing osteoclastogenesis. Such findings are further supported by evidence that estrogen supplementation to elderly women dramatically reduces bone loss, and the concentration required for sustaining relatively normal bone

remodeling is lower than level required for stimulating known targets such as breasts and uterus (6). Numerous studies have shown that estrogen level is inversely proportional to risk of bone fracture. Interestingly, the sensitivity of skeleton to estrogen seems to increase as age increases. In a study with ovariectomized mice, it was found that the uterus has a greater sensitivity to estrogen than bone in 3-month-old mice, this phenomenon, however, was reversed in 6-month-old mice (9). In addition, recent studies also suggest that estrogen may play a direct role in osteoclastogenesis. According to a study done by Kameda et al, estrogen is found to directly inhibit bone resorbing activity of osteoclast through the estrogen receptor  $\alpha$  found on the surface of osteoclasts (10). This inhibitory effect was able to be suppressed after neutralization with antiestrogen (10).

## **1.2. RANK/RANKL/OPG in Osteoclastogenesis and Their Potential as Antiresorptive Therapy Target**

Osteoclasts are multinucleated cells resulting from fusion of their mononuclear progenitors from macrophage/monocyte lineage (11). They are thought to be the major contributors to bone resorption. As osteoporosis is a consequence of unbalanced bone resorption and bone formation, osteoclasts are targeted by many pharmaceutical agents in trying to slow or halt their bone resorption activity. However, osteoclasts and their differentiation mechanism were not clearly understood until recently with the discovery of macrophage colony-stimulating factor (M-CSF), and most importantly receptor for activation

of nuclear factor  $\kappa$  B (RANK), its natural ligand (RANKL) and osteoprotegerin (OPG).

Before the discovery of these cytokines, it was known that osteoclastogenesis is not an independent process and, in fact, required the presence of osteoblasts or their precursors at close proximity (11-13). While numerous cytokines have been suggested to regulate osteoclast function, general understanding was not revealed until the identification of M-CSF and RANKL (12, 14). While both M-CSF and RANKL are important for the generation of functional osteoclasts, M-CSF, which is secreted by osteoblasts, was found to play an important role in early proliferation and differentiation of osteoclasts. In a 6-day culture of osteoclast progenitors, it was found that with M-CSF and RANKL, the progenitors undergo proliferation in the first 4 days and differentiation in the last 2. However, when M-CSF was removed from culture either during the proliferation or differentiation phase, osteoclasts failed to form (12). Interestingly, there is evidence that estrogen inhibits the expression of M-CSF, which may contribute partially to the initiation of bone loss for postmenopausal women (11).

RANKL, also termed OPG ligand, osteoclast differentiation factor and TNF-related activation-induced cytokine (TRANCE), was first identified as OPG's natural ligand and can be found in three different forms – primary secreted protein, 317-amino acid cell-bound protein, and an enzymatically cleaved truncated form of the cell-bound protein (14, 15). RANKL can be expressed by many cell types including osteoblasts, osteoclasts, chondrocytes and endothelial

cells. Before truly realizing the mechanism, RANKL was shown to be necessary and, in the presence of M-CSF, sufficient to differentiate osteoclast precursors cell into mature osteoclast by inducing gene expression of important receptors and enzymes such as tartrate-resistant acid phosphatase (TRAP), calcitonin receptor and cathepsin K (16, 17). It was found that in the absence of RANKL, M-CSF is only capable of generating mononuclear cells with no bone resorbing activity. Added to the fact that RANKL alone cannot induce osteoclast maturation, it has long been suggested that M-CSF may induce a receptor for RANK on osteoclast, which in turn provides a site for RANKL to exert its function.

OPG is a 401-amino acid protein, which exists only in a soluble secreted form, and helps with the discovery of RANKL. It was discovered independently in 1997 by two groups – Amgen in the US and Snow Brand Milk Group in Japan (16). Although OPG mRNA was found to be expressed in many other tissues such as heart, lung, kidney, liver, spine and bone, most of OPG's activity was reported in bone while its action in other tissues is yet to be determined. Although the mechanism was initially not known, OPG was believed to inhibit osteoclast differentiation. In OPG-overexpressing transgenic mice, the BMD increased significantly and only a low number of osteoclasts were found (18). On the other hand, in OPG-deficient mice, the bone porosity was found to be even greater than those with osteoporosis (18, 19). Upon the discovery of RANKL, it was determined from numerous studies that OPG is able to accomplish this inhibitory effect by acting as a decoy receptor for RANKL in the extracellular matrix, thus preventing RANKL from exerting its biological action (15, 18, 20-22).

The identification of OPG and RANKL provided a good direction that leads to the last piece of the puzzle. Since OPG is able to neutralize RANKL and prevent its binding to osteoclasts, it was logical that osteoclasts and their precursor cells must express a receptor for RANKL. This receptor, later identified as RANK, was soon discovered. In bone marrow-derived osteoclast progenitors and mature osteoclasts, a high level of RANK mRNA expression was found. A study with RANK knock-out mice provided concrete evidence that RANK is the only receptor for RANKL as these mice suffered from osteopetrosis due to lack of osteoclasts (16). In a recent cell-based study using murine macrophage cells, osteoclast formation and bone resorption was successfully inhibited by using siRNA knock-down of RANK (23). Both of these results further confirm the importance of RANK in initiating and regulating osteoclast activity.

Following the discovery of the triad of RANK, RANKL and OPG, the regulation of osteoclastogenesis has become clearer. It became evident that osteoclastogenesis is closely regulated by osteoblasts since the promoter region of both RANKL and OPG contain binding sites for osteoblastic transcription factor *cbfa-1*, which is essential for osteoblastic differentiation and function of bone (14). In *cbfa-1*-deficient mice, both osteoblasts and osteoclasts are absent. This suggests that osteoblasts closely regulate osteoclasts within the BMU to specific site for bone resorption. Interestingly, in osteoblastic precursor cells, it was found that RANKL is expressed at high levels while OPG is secreted at low levels. This high RANKL-to-OPG ratio favors osteoclastic generation and activity. On the

other hand, as osteoblasts mature, this ratio reverses and osteoclast activity is in turn reduced or lost (14).

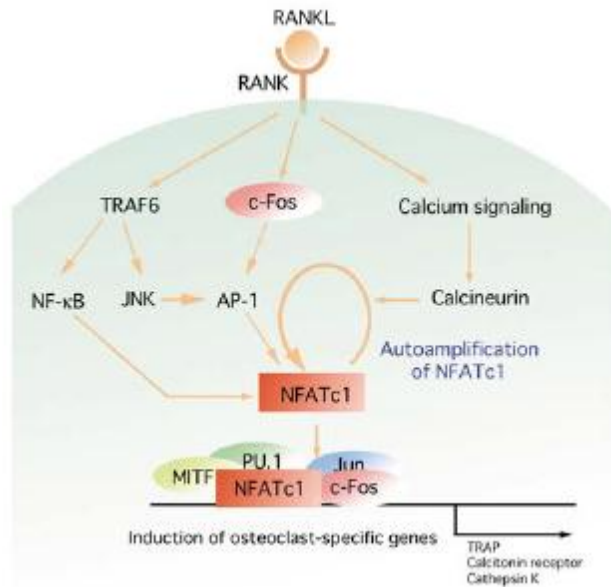


**Figure 1.7 Signaling Cascade Initiated by RANKL. The true regulator of osteoclastogenesis is thought to be NFATc1, which can be induced by various RANKL-initiated pathway. Image taken from Takayanagi 2005 (13).**

In summary, osteoclastogenesis requires first the binding of M-CSF, which is secreted by pre-osteoblast or stromal cells. This provides the survival signal for osteoclast precursors and upregulates their expression of RANK and increases the number of RANK molecules presented at the cell surface (12, 16). Subsequently, RANKL, which can be found either in soluble form or in cell-bound form on pre-osteoblasts, binds to RANK or soluble OPG decoy receptor (12, 17, 24). The number of osteoclast precursor cells being differentiated into osteoclasts is inversely proportional to the amount of OPG present. The cell-bound form of RANKL on pre-osteoblast is consistent with the previous findings that these cells need to be in close contact with osteoclast precursors in order to

permit osteoclastogenesis. Once RANKL has successfully bound to RANK, a series of signaling cascades commence for cell differentiation, and the mononuclear osteoclast precursors start to fuse and form the multinuclear osteoclasts (17). While their functions are not entirely known, the activation of RANK from RANKL induces multiple cytokines such as TNF receptor associated factor (TRAF6), which in turn activates multiple pathways such as mitogen-activated protein kinase, Akt and NF- $\kappa$ B, and c-Fos, which activates activator protein 1 (AP1), a transcription factor complex consisting of multiple units activated by TRAF6 (13, 25). However, later research reveals that although these cytokines are essential, they are not sufficient and not directly responsible for initiating osteoclast differentiation.

To further investigate the specific cytokine responsible for RANKL-induced osteoclast differentiation, Takayanagi et al performed a genome-wide screening to identify specific genes induced by RANKL (13). Such effort resulted in the discovery of transcription factor NFATc1, a transcription factor gene that is most strongly induced after RANKL stimulation (13). Mutant NFATc1 stem cells were found to be incapable of undergo osteoclastogenesis. Further research showed that induction of NFATc1 by RANKL is via c-Fos and TRAF6, which are also activated during RANKL induction (13). During the terminal differentiation stage, NFATc1 is found to form a complex with c-Fos and AP-1 and binds to the promoter of osteoclast-specific gene such as TRAP and calcitonin receptor (13). Therefore, NFATc1 is considered as the master regulator in osteoclastogenesis and it is often used as a gene expression marker for osteoclastic activity.

Further studies have been done on the exact nature of the binding of RANK and RANKL. Similar to other receptor in the TNF family, although the molar ratio of binding between RANK and RANKL is 1-to-1, a binding of RANK-trimer and RANKL-trimer is necessary in order to successfully generate signaling cascade and form fully functional osteoclast (26). However, there has been continuous debate on the order of this trimerization. While the general consensus is that RANKL first trimerizes, binds to RANK, which in turn brings 2 units of RANK within close proximity to initiate trimerization, there have been other research suggesting that RANK is capable of trimerizing without the aid of RANKL (24, 26). Despite the fact that the ongoing debate on the order of RANK/RANKL trimerization, it is certain that the activation of RANK/RANKL is not an “all-or-none” threshold effect. That is, dimerization of RANK and RANKL is also capable of inducing a signaling cascade, but the resulting effect is much less significant in that the resorption activity and expression of osteoclast markers normally induce by RANKL are greatly reduced (27).

With the mechanism of osteoclastogenesis now generally understood, it has opened up new targets for the pharmaceutical industry to develop antiresorptive agents. Denosumab, developed by Amgen, is a human monoclonal antibody that acts similarly to OPG. It is an anti-RANKL antibody that successfully inhibits bone resorption by neutralizing RANKL and preventing it from binding to RANK for osteoclastogenesis. Since a RANK trimer is required for complete osteoclastogenesis, disrupting the trimerization process may also prove to be potential therapeutic strategy. Combining the number of cytokines

involves in osteoclastogenesis and the power of biotechnology today in generating antibody therapeutics, the discovery of osteoporosis therapeutics that are both safe and potent is more than likely.

### **1.3. Current Treatment in Osteoporosis**

Since osteoporosis is characterized by the imbalance of bone remodeling, in particular increased bone resorption and decreased bone formation, treatments for osteoporosis can be classified into 2 categories based on their respective approaches – anabolic and antiresorptive.

#### **1.3.1 Anabolic Agents**

Anabolic reagents aim to promote bone formation to re-balance the bone remodeling. In the past, sodium fluoride was used as it was found to stimulate bone formation and increases bone density in osteoporotic women (28). However, this treatment comes with many disadvantages – Firstly, co-administration of calcium is necessary in order to minimize mineralization defects and increases in bone resorption that is caused by other action of fluorides. Moreover, a significant population of patients being administered with sodium fluoride experienced gastric irritation and other gastric side effects. Most importantly, although sodium fluoride increases mineral bone density, bone with excess fluoride content has an abnormal structure and increased risk of fracture, which defeats the purpose of preventing fractures in osteoporosis patients (28).

Osteoblasts generate a number of cytokines to promote their own proliferation. Factors such as insulin-like growth factors I and II and transforming growth factor  $\beta$  are all capable of promoting osteoblast proliferation, are available in recombinant and purified form, and can be used as anabolic agents to stimulate osteoblast formation and in turn increase bone formation. However, such growth factors are involved in many cellular signaling pathway and exhibit potent extraskeletal effects, which may generate unwanted side effects if used as an anabolic agent (28).

The first clear and relatively safe anabolic therapy that stimulates bone formation is parathyroid hormone, or PTH (2). Clinical trials have been done using full intact 84 amino acid-PTH and the truncated 34 amino acid-peptide, known as teriparatide. In a phase III clinical trial with teriparatide at 20 $\mu$ g dose with over 1600 postmenopausal women, results showed that there was a 65% reduction of chance of new vertebral fracture and 53% reduction for non-vertebral fracture (2). However, there is evidence suggesting that the outcome of PTH treatment can be affected by prior antiresorptive treatments. In patients who were previously treated with alendronate, a bisphosphonate antiresorptive drug, bone mineral density was unchanged after PTH treatment. On the other hand, patients treated with raloxifene previously did not have any effect compared to the treatment-naïve patients when they were administered PTH (29).

Strontium ranelate could be another promising anti-osteoporotic agent that resembles an anabolic agent (2). Although it is suggested to promote bone formation and reduce bone resorption, its exact mechanism of action is still

unclear (2). In various large-scale phase III clinical trials, strontium ranelate has found to reduce vertebral and non-vertebral fracture risk significantly. Moreover, strontium ranelate is found to be well-tolerated with only a small population of the patients having gastrointestinal side effects and an unexplained increased risk of venous thrombosis (2).

### **1.3.2 Antiresorptive Agents**

As the term suggests, antiresorptive agents are therapeutics that try to reduce osteoclast activity in bone resorption and they account for most of the market share in treatment against osteoporosis today. These agents include estrogen, selective estrogen receptor modulator (SERM), calcium and vitamin D, calcitonin, bisphosphonates and recently developed monoclonal antibody therapeutics.

Estrogen replacement therapy has long been considered as a first line prevention and therapy for postmenopausal osteoporosis because its deficiency in women after menopause is one of the major causes of osteoporosis. Since it is widely believed that the majority of bone loss occur during the first 3-6 years after menopause, estrogen therapy is most effective when it is initiated soon after menopause (8, 28). In early postmenopausal women, estrogen therapy has been found to increase spinal BMD by 3 to 4% and hip BMD to a similar extent was induced by bisphosphonate therapy (8). It was also found that early estrogen therapy decreased subsequent osteoporosis-related fractures by as much as 50% (28). While women who have undergone hysterectomy can be treated with estrogen alone, others are usually co-administered with progestin because

estrogen therapy is found to be associated with several risks (30). Without the co-administration of progestin, women with estrogen therapy alone are found to have an elevated risk of uterine cancer. Moreover, there is also evidence that estrogen therapy may increase the risk of breast tumours from 20 – 50% (8).

As mentioned above, estrogen can directly act on inhibiting osteoclastic activity by interacting with the estrogen receptor  $\alpha$  found on osteoclasts. As such, the discovery and development of a set of compounds that is able to exert full or partial agonistic effect of estrogen lead to a new class of antiresorptive therapeutic agent known as selective estrogen receptor modulator, or SERM (8). Each SERM is required to have strong binding affinity to estrogen receptor, but they are unique in that their molecular structures dictate their individual tissue-selective pharmacology (8). There are also speculations that different combinations of SERM-receptor complexes are able to recruit different cytokines depending on the tissue types, thus the ability of SERM to exhibit both antagonist and agonist effect at different tissue (8). For example, while raloxifene and tamoxifen act as antagonist in breast and serve as treatments for breast cancer, they both exert various degrees of agonistic activity in bone (30). Although the exact mechanism of action is still unclear, SERMs are thought to act similarly to estrogen in that upon binding to the surface estrogen receptor, SERM blocks the production of cytokines required for osteoclast differentiation (8). The 2 most well-known SERMs are tamoxifen and raloxifene. In the case of tamoxifen, it is only found to be a partial agonist in bone. With the additional side effect of elevated risk of uterine cancer, it is discouraged as a treatment option for postmenopausal

osteoporosis (8, 30). On the other hand, administration of raloxifene to early postmenopausal women has been found to prevent bone loss at all skeletal sites. In a clinical trial with postmenopausal women, even though raloxifene increases only 3 to 4% in bone density, it was able to reduce the risk of vertebral fractures by 40% (8). Although raloxifene therapy does come with a slight elevated risk of venous thrombosis similar to estrogen therapy, its potent antiresorptive effect as well as its potential to prevent breast cancer may encourage the use of this SERM in the future (2). Other than the demonstrated potency of some SERMs on osteoporosis, the idea of using receptor agonist also created a new therapeutic strategy for osteoporosis, as seen in the case of the development of the monoclonal antibody antiresorptive agent.

Calcium and vitamin D are both important nutrients in maintaining healthy bone. Even though it is known insufficient that calcium level leads to bone loss, calcium supplementation alone has demonstrated minimal effects on BMD in both early and late postmenopausal women (30). On the other hand, vitamin D deficiency has been associated with reduced BMD, increased bone turnover, and increased risk of hip fracture (2). Numerous clinical trials have revealed results that the combination therapy is more significant in reducing fractures in elderly women with vitamin D deficiency, but no significant improvement in postmenopausal women without a vitamin D deficiency (30). In addition, in a report of the Women's Health Initiative, a 15-year megatrial carried out by the National Institutes of Health, its finding in calcium/vitamin combination treatment in over 36000 postmenopausal women, the results reached a similar conclusion

(2). With many of these discouraging results, calcium and vitamin D are now mostly used as supplement in combination with other antiresorptive treatment such as bisphosphonates (2).

Calcitonin is a peptide hormone that is produced by thyroid C cells and is found to possess antiresorptive activity by inhibiting osteoclastic activity directly (8, 30, 31). This antiresorptive peptide is found to be less effective in preventing cortical bone loss than cancellous bone loss in postmenopausal women (30). Although pig, eel, human and salmon calcitonin are all used therapeutically, salmon calcitonin is found to be the most potent and has minimal immunogenicity and side effects when given at low dosage intranasally (8, 28, 30, 31). Although there are minimal immediate side effects from the salmon calcitonin administration, the use of peptide hormone as therapeutics has historically raised some concerns – First, long-term administration of hormone may result in calcitonin-induced loss of calcitonin receptor, otherwise known as hormone-induced resistance. In addition, continuous administration of non-human peptide may also generate endogenous anti-salmon calcitonin antibody production that may neutralize and decrease the effect of salmon calcitonin (28, 30).

Bisphosphonates are by far the most successful and effective class of antiresorptive agents used in treatment of metabolic diseases such as osteoporosis (8). They are compounds structurally similar to inorganic pyrophosphate (PPi), which is an endogenous molecule that acts as a critical physiological inhibitor of bone mineralization (28, 32). Unlike the endogenous PPi where the two phosphate atoms are linked by an oxygen atom to form an unstable P-O-P bond,

bisphosphonates are much more stable where the phosphates are linked by a carbon atom, forming a P-C-P bond (8, 28, 30, 32). Various bisphosphonates were synthesized by substituting one or both hydrogen atoms on the carbon atom. Since they are structurally analogous to PPI, bisphosphonates are also capable of binding divalent ions such as  $\text{Ca}^{2+}$ ,  $\text{Mg}^{2+}$ , and  $\text{Fe}^{2+}$  by coordinating one oxygen atom from each phosphate group. The binding to  $\text{Ca}^{2+}$  ions is further improved by substituting one of the hydrogen atoms in the central carbon with either a hydroxyl- or amino- side chain, which allows an additional electronegative atom to bind to the metal ions (32). Due to their high affinity for  $\text{Ca}^{2+}$  ions, bisphosphonates have very high affinity to hydroxyapatite bone mineral surfaces, which is the basis of their clinical significance (30, 32). In various radiolabeled studies, bisphosphonates are found throughout the bone surface, but are particularly concentrated in areas where there is osteoclastic activity (32), which is a good indicator that bisphosphonates exert effects on osteoclasts directly.

Bisphosphonates can be further classified into two classes based on the chemical composition of the side chain – The first generation are non-nitrogen-containing molecules, while the second generation are more potent, nitrogen-containing molecules. While both classes of bisphosphonates act directly on osteoclast and have the ability to perturb intracellular metabolism and induce osteoclast apoptosis, the routes of achieving such effects are different between the two generations. First generation bisphosphonates such as clodronate, etidronate and tiludronate closely resemble PPI structurally and, in turn, inhibit osteoclastic activity by incorporating metabolically into non-hydrolyzable analogues of ATP

due to the more stable P-C-P bond (32). These non-hydrolyzable analogues will then accumulate within osteoclasts, preventing their normal function and causing cellular apoptosis. Second generation bisphosphonates such as alendronate, risedronate, zoledronate and ibandronate still contain a stable P-C-P bond, but they do not inhibit osteoclast activity by metabolizing into non-hydrolyzable ATP analogues. This class of molecules is thought to act as transition state analogues of isoprenoid diphosphates and inhibit the mevalonate pathway (32, 33). The mevalonate pathway is a synthetic pathway for endogenous isoprenoid compounds, which are critical for post-translational modifications for GTPases. Therefore, inhibition of the mevalonate pathway will most likely result in partially or non-functional GTPases and play a negative effect on the signaling pathway for osteoclastic activity (32, 33). In clinical studies, first generation bisphosphonates generated encouraging results with successful but small increases in bone mineral content and also decreases in fracture risk (34, 35). On the other hand, clinical studies with second generation such as alendronate generated encouraging results, where it was the first bone resorption inhibitor to show significant reduction of fracture risk by roughly 50% in both spine and hip in a large randomized trial (8). Although bisphosphonates have substantial side effects such as upper gastrointestinal distress, new more potent drugs are being developed to try to reduce the effective dose required and reduce side effects. One of the disadvantages of bisphosphonates are their low bioavailability (~5%), however its superb binding affinity to bone is able to offset this disadvantage in that bisphosphonate can be found on bone surface even after several years (28,

30). Given the substantial effectiveness of bisphosphonates over other available treatments, bisphosphonate is by far the most popular treatment and it is used for treating the majority of osteoporotic patients (8).

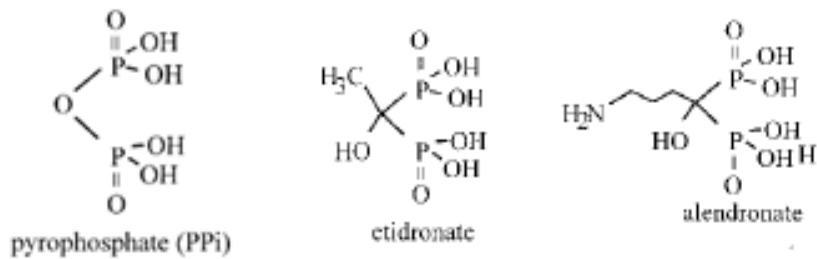


**Figure 1.8 Chemical Structure of Endogenous Pyrophosphate and Bisphosphonates.** While the two phosphorus atoms are linked by an oxygen atom, they are linked together by a more stable carbon atom in bisphosphonate. Etidronate is considered as the first generation, non-nitrogen-containing bisphosphonate. Alendronate is regarded as the second generation, nitrogen-containing bisphosphonate.

Monoclonal antibodies are a new strategy of antiresorptive therapy that was made possible by recent advances in antibody biologics generation. The most notable and successful agent of this class is Denosumab developed by Amgen, which was approved by the FDA in 2010. It is a human monoclonal antibody with binding affinity against RANKL (36-39). Since RANKL is essential in the RANK, RANKL and OPG pathway for osteoclastogenesis, Denosumab is able to achieve its antiresorptive effect by mimicking the molecular action of OPG and blocking the binding of RANKL to RANK, in turn inhibiting osteoclastogenesis, decreasing bone resorption and increasing BMD (38, 39). Various clinical studies have shown that Denosumab is able to significantly increase BMD and decrease fracture risk in vertebral, nonvertebral and hip (36, 39). However, unlike

bisphosphonate treatment where patients' BMD remain unchanged after treatment is withdrawn, BMD immediately decreases after the termination of Denosumab treatment (37). This observation is reversible in that BMD significantly increases again after retreatment with Denosumab. With low incidence of side effects comparing to substantial gastrointestinal distress experienced by some in bisphosphonate treatment, Denosumab has demonstrated the potential for a brand new class of antiresorptive agent, in which monoclonal antibodies against a specific cytokine can be used to disrupt the signaling cascade of any pathways involving bone resorption by osteoclast.

Other classes of molecule that are being explored as antiresorptive agents include cathepsin K inhibitor, which inhibits lysosomal cysteine proteinases that are highly expressed in osteoclasts and are thought to degrade type I collagen (8, 40). Alfacalcidol and calcitriol, which are vitamin D analogues, are also used in some countries for treating osteoporosis even though they have been shown to lead to minimal increases in spinal BMD (30). Overall, it is evident that there are many more available antiresorptive therapeutics in the current market than anabolic agents. This may be due to the tendency of anabolic agents to be endogenous hormones or their analogues. As such, there are often reported side effects such as unwanted androgenic actions, change in plasma lipoproteins and, when given orally, hepatic dysfunction (28).

## **1.4. Bone-turnover Markers**

During bone remodeling, both bone formation and resorption processes are active to various degrees. As a result, key enzymes and by-products of these processes are constantly being produced or released into the circulation (41-49). These biochemical molecules, termed bone turnover markers, are often used to determine the rate of bone formation or bone resorption by measuring enzymatic activity of osteoblasts or osteoclasts, or measuring the level of the by-products being released into the circulation (46-50). Logically, bone turnover markers are classified into bone resorption markers and bone formation markers (41, 43-45, 47, 49). Although numerous studies have shown that the levels of bone turnover markers are strongly correlated to actual rate of bone turnover, it should be noted that these markers do not generate information on the actual rate of bone turnover. Each bone turnover marker can only provide information on one aspect of bone resorption or bone formation and their level can be affected by the uneven contribution of cortical and trabecular bone remodeling (42, 43, 45, 46, 49).

### **1.4.1. Bone Resorption Markers**

With the exception of tartrate-resistant acid phosphatase, most bone resorption biochemical markers are degradation product of bone collagen (41, 43-45, 47, 49, 51). Hydroxyproline is a modified form of the amino acid proline and it constitutes 12-14% of the total amino acid content of mature collagen (42, 44, 45, 51). Its main function is to stabilize the triple helix structure of collagen and only approximately 10% of the hydroxyproline is excreted through urinary

excretion in either free or peptide-bound form (44, 45, 47, 49). Interestingly, although hydroxyproline is used exclusively as a bone resorption marker, it is excreted through degradation of extracellular as well as newly synthesized collagen (41-43, 47, 48, 51).

Other common bone resorption markers used are Collagen type 1 crosslinked N-telopeptide, or NTX, and Collagen type 1 crosslinked C-telopeptide, or CTX (41-45, 47, 49). Both of these markers are breakdown products of type I collagen resulting from bone resorption by osteoclasts (42, 43, 47). They are among the most widely-used bone resorption markers and there are numerous immunoassay kits in the market for testing either serum or urine samples (42, 43, 47). Since both of these markers are the direct result of bone resorption, their level decreases significantly after antiresorptive therapies (42). Urine measurement of NTX and CTX has the advantage of overcoming variability due to dietary intake (42). In recent years, studies have shown that the ratio of  $\alpha$ CTX to  $\beta$ CTX further accurately reflects the true bone turnover rate (42). The reason is that the C-terminal telopeptide of the  $\alpha$  chain of collagen is found to undergo constant  $\beta$ -isomerization or racemization, which is an age-dependent process (42, 43). As such, the  $\alpha$ CTX/ $\beta$ CTX ratio will be increased in people with very rapid bone turnover of newly synthesized bone.

Pyridinoline (PYD) and deoxypyridinoline (DYP) are also two bone resorption markers formed from the activity of osteoclasts (41, 42, 45, 47)(47). These two markers can be found in either free or peptide-bound form, and are nonreducible crosslinks found in mature collagen, with PYD mostly found in

cartilage, bone, ligaments and vessels and DYD found in bone only (41, 42, 45, 47). There are in general two ways of detecting these crosslinks – 1. HPLC, which was developed early and continues to serve its purpose of performing accurate detection with continuous improvement in the instrumentation. 2. Immunoassay, which was developed recently and is often preferred since it is thought to provide an even more accurate result than HPLC (41, 42, 45, 47). One of the most significant advantages of PYD and DYD, as markers, is that their levels are independent of newly synthesized collagen as well as dietary collagen, which greatly increases the sensitivity and decreases the variability of detection (41-43, 45).

Of all the commonly studied bone resorption markers, Tartrate-resistant acid phosphatase, or TRAP, is the only commonly-used enzymatic marker. It is a lysosomal enzyme and is the only marker that directly reflects osteoclastic activity (42). While there are many TRAP isoforms, TRAP5b is most specifically expressed on osteoclast (42). TRAP level typically increases with increased bone turnover and it can be measured either by an enzymatic activity assay or recently developed immunoassay (42, 47). However, TRAP activity assay contains some major disadvantages: Specificity of TRAP enzymatic assay of serum samples is low because TRAP is expressed in other cells; TRAP activity can be inhibited by various substances within serum; TRAP activity can also drop by freeze-thaw cycles (42, 45, 47). Due to these reasons, TRAP5b-specific immunoassay is much preferred over enzymatic activity assay (42, 45, 47).

Other than the above mentioned bone resorption markers that are widely accepted and utilized for conducting studies in bone turnover, there are other bone resorption markers reported, such as carboxyterminal telopeptide of type 1 collagen (ICTP), bone sialoprotein (BSP), fasting urinary calcium, cathepsin K and hydroxylysine glycosides (41, 43, 46, 47). However, they are not commonly used due to their poor sensitivity or large variability.

#### **1.4.2. Bone Formation Markers**

Comparing to bone resorption markers, there are considerably fewer bone formation markers reported. They are either direct or indirect products resulting from osteoblastic activity (45). It should be noted that all bone formation markers' level are measured in serum or plasma (45).

Alkaline phosphatase (AP) is an enzyme with 50% of the activity in serum derived from liver and the remaining half from bone (45). AP that originates from bone resides in the plasma membrane of osteoblasts and sheds into the circulation (41). Although the exact function is not completely clear, AP is known to be crucial for osteoid formation and mineralization (42, 45). AP is similar to the TRAP5b mentioned above because not only can they both be detected by enzymatic activity assay and isoform-specific immunoassay, but they also share the same disadvantages in the enzymatic activity assay detection methods – Since 50% of serum AP activity originates from liver, results generated from AP activity assay are often questioned and not accepted (41, 42, 45, 47).

Osteocalcin, also known as bone-gla-protein, is a hydroxyapatite-binding protein produced specifically by osteoblasts. Although its function is not

completely understood, it is one of the most widely used bone formation marker (41-43, 45, 47). With its high bone affinity, most osteocalcin synthesized is integrated into bone, with only minor amounts being leaked into the circulation (42). Since it is not an enzyme, osteocalcin can be detected only by immunoassay. Despite osteocalcin's specificity to osteoblast and bone formation, there is one drawback in using this marker to gauge rate of bone formation – Osteocalcin undergoes rapid degradation in serum and with the antibodies of commercial immunoassay kits only detecting certain fragment of the markers, the co-existence of intact and fragmented osteocalcin greatly increases the variability of the assay (41-43, 45, 47, 51). However, due to the lack of promising bone formation marker available, osteocalcin remains one of the most commonly used bone formation markers.

Another set of bone formation markers are derived from procollagen type 1 propeptides, which are secreted by osteoblast into the extracellular space (41). The amino- and carboxy-terminal propeptides of type 1 collagen (P1NP and P1CP respectively) are generated in an equimolar ratio from post-translational cleavage of type 1 procollagen molecules by propeptidases before assembly into fibrils (42, 43, 45, 47). The fragments of these molecules that are released into the circulation can then be detected as markers by various forms of immunoassay (45). Although both P1CP and P1NP have the same origin, P1CP is not preferred because it is cleared by the mannose receptor, which can be affected by various hormonal regulation pathways, thus complicating result (45).

### **1.4.3. Benefits and Limitations of Bone Turnover Markers in Diagnosis of Osteoporosis and other Bone-Modifying Diseases**

With numerous markers available to generate information on different aspects of bone turnover rate, these bone-turnover markers are valuable in the investigation of bone-modifying diseases such as osteoporosis, as well as the evaluation of the effectiveness of therapeutics. In particular, bone turnover markers are especially useful in post-menopausal osteoporosis and Paget's disease, where both of these diseases have significant increase in bone turnover (46). In turn, any therapeutics that have an impact on these diseases should, in turn, cause a significant change in bone turnover marker levels (52). In many clinical situations, bone turnover markers are used to monitor patients' conditions as well as the effectiveness of their treatment (44, 46, 52-56). In some clinical trials, bone turnover markers are even used as surrogates for a clinical end point that is otherwise hard to measure (55). In laboratory settings, bone turnover markers are constantly used as an indicator of drug effectiveness in animal and cell-based studies (57, 58). Although the uses of bone turnover markers are diverse, there are still no strong correlations between bone turnover marker levels and bone mineral density, prediction of fractures and selection of treatments, especially in the case of post-menopausal osteoporosis (53).

### **1.5. Antibody Biologics and their Value as Therapeutics**

Antibodies are nature's way for the human immune system to fight foreign threats such as bacterial and viral infections and toxins. Antibodies are highly

specific to their intended target and these antigen-specific antibodies are selected from a large repertoire ( $10^{10}$ - $10^{12}$ ) of possible variants (59). These highly-specific antibodies are amplified within the human body when the threat is present and can trigger responses such as neutralizing biological activity, promoting target degradation and triggering signaling cascades for cell-mediated cytotoxicity as defense mechanism (59).

The human antibody (immunoglobulin) is a Y-shaped molecule (~150kDa) that is made from two identical heavy and light chains, where each chain is subdivided into constant and variable regions (59). These two chains are linked strongly together by multiple disulfide bonds. Each of these regions serves its own purposes – The variable region, in particular the 3 solvent-exposed hypervariable loops at the tip of the molecule known as the complementary determining regions (CDRs), is responsible for enabling specific binding affinity to a target antigen, whereas the constant region is responsible for signaling defense mechanisms such as cell-mediated cytotoxicity (59, 60).

There are five different known classes of human immunoglobulins, IgA, IgD, IgE, IgG and IgM, with each of them participating in a different role (61). IgG, however, is often referred to as “therapeutics antibody”. IgG, depending on the subclass, has the longest plasma half-life from 7 – 23 days of all 5 immunoglobulin classes (59). In addition, although the 4 IgG isotypes possess very similar sequence, they are able to trigger very different signaling cascades for cell-mediated responses (59-61). This characteristic allows the selection of

subclass prior to antibody development based on the preference of which mechanism is required to achieve therapeutic effect (60).

Even though the therapeutic value of antibodies was long known, it was not made possible until the development of hybridoma technology by Kohler and Milstein (59, 62, 63), who deservedly won the Nobel Prize because of this discovery, in 1984. This technology enables the fusion of pre-immunized mouse B-cells and myeloma cells to generate an immortal cell line (hybridoma) that can be grown in tissue culture and provide a continual source of antigen-specific antibody (62, 63). This technique led to the development of the first monoclonal antibody, Orthoclone OKT3 by Johnson & Johnson Therapeutics in 1986 for organ transplant rejection (59, 62). Since then, the field of antibody therapeutics has taken flight and evolved to be an important segment of the pharmaceutical industry. As of 2005, there are 20 FDA-approved monoclonal antibodies therapeutics on the market and accounted for an annual sale of \$14 billion US dollars (62). A survey was conducted by Business Communications Company in 2005 and it was shown that of the 200 biopharmaceutical companies being surveyed, there were approximately 500 antibody-based development programs (62). Due to an antibody's specificity to a particular antigen, antibody therapeutics are now developed for a wide range of indications, such as rheumatoid arthritis (64, 65), various forms of cancer (38, 66-68), osteoporosis (30, 36-39), asthma (62) and macular degeneration (62). It should be noted that many of these antibodies carry out their function via many different pathways – while some may simply neutralize secreted toxins from infectious agents, others can scavenge and

bind to important cytokines and prevent unwanted cellular pathways such as cancerous tumour proliferation (59). Other than therapeutics, antibodies are also utilized in diagnostic such as immunoassays where an antibody is generated for the purpose of detecting a specific antigen. In recent years with the advancement of imaging technology, there has also been an increasing interest in employing antibodies as molecular probes for cell-based and even in vivo imaging platform, with a particular interest in various types of cancer (69).

Although antibodies possess much potential in the field of therapeutics and diagnostics, there were many issues that needed to be overcome. The most problematic concern in the early days was the immunogenic responses to mouse antibodies generated from hybridomas when these are administered to human (62). In an attempt to prevent such unwanted response and to make the therapeutic antibodies more suitable for human administration, several sequential approaches were made. The first approach was to fuse the human constant region with the mouse antigen-specific variable region to generate a “chimeric” antibody, in which approximately 70% of the antibody’s sequence was homologous to human IgG sequence. The next approach aimed to further increase the percentage of homology by moving the CDRs isolated from the antigen-specific mouse antibody and inserting these regions into a human IgG antibody (62), thus creating the “humanized” antibody. Despite this approach achieving a homology of up to 95%, immunogenicity still occurred at a low level and there was still a need to create a fully human antibody (62). Therefore as a third approach, several platforms were developed to generate fully human antibodies, these included the

“Xenomouse” technology, where mice were genetically engineered to have their immune system removed and replaced by the human immunoglobulin repertoire; the human “morphodoma”, where in vitro immunized human B-cells were used to yield fully human antibodies from human hybridomas; and phage technology, where the immunoglobulin genes from B-cells were used to construct a human phage library (62). One of many successful therapeutic antibodies generated by the xenomouse technology is Denosumab by Amgen, which is an antiresorptive agent for treating osteoporosis and other metabolic bone diseases (36).

While the first two platforms yield IgG monoclonal antibodies, the last mentioned platform, the phage technology, has opened up a brand new field of creating antibody therapeutics, which will be discussed below. Although the problem of immunogenicity of antibody has been overcome, there are still other issues preventing antibody therapeutics from widespread application – The current antibody therapeutics in late-stage development target cell surface receptors and soluble factors such as growth factors or toxins, but in order to maintain antibody’s role in biopharmaceutics, there is a need for developing antibodies that can target other biomolecular species such as multi-transmembrane receptors, channel proteins and even intracellular targets (62). In addition, the timeline from discovering and developing attractive antibody candidates into clinical trials to developing large-scale production for commercialization is still longer than desired. This provides hurdles to many companies as it not only increases the development cost, but also decreases companies’ financial benefits from the patent as generic biopharmaceutics will soon become competitors if

companies require majority of the patent protection period for developing the antibody therapeutic (62).

### **1.5.1 Engineered Antibody Fragments**

While the manufacturing and production process of monoclonal IgG antibody continue to morph and improve, there is another branch of antibody therapeutics on the horizon – With the advances in biotechnology and genetic engineering, there has been an increasing popularity of using antibody fragments instead as therapeutic and diagnostic agents. These engineered fragments include Fabs, single chain variable fragments (scFv) and domain antibodies (dAbs) (59).

Since an antibody can be divided into various domains, scientists have taken advantage of this finding and have expressed the antigen-binding variable region independent of the constant region. Since the constant region of IgG is responsible of mediating cell cytotoxicity mechanism, despite having fully functional antigen-binding site, fragments with the removal of the constant region can only serve the purpose of neutralization, imaging or site-directed drug delivery (59). Fabs are the biggest of the fragments (~50kDa) consisting of the variable regions and part of the constant region with only the constant regions at the stem of the Y-shaped IgG molecule being removed (59). The fragment is connected by a disulfide bond and the remaining constant domain is believed to help with protein folding and stability (59). On the other end of the spectrum, dAbs are the smallest of the fragments (~15kDa) consisting of either the variable region from the heavy chain or from the light chain (59). As a result, dAbs contain only 3 CDRs as compared to 6 found on an IgG.

Single chain variable fragment (scFv), the fragment used for this project, is a heterodimer of the variable regions from heavy and light chain and has a molecular weight of approximately 30kDa (59, 61). The 2 variable regions are linked together by a polypeptide linker composed of glycine and serine in a 4:1 ratio (59, 61). While the linker is usually 12-15 amino acid long, a shorter linker will prevent the heavy and light chain to interact in forming a monomer and in turn facilitate the association with a second scFv monomer, forming a bivalent dimer known as dibody (59). Since scFv is only held together by a polypeptide linker, varying amounts of dimers and higher degree of oligomers will be present in equilibrium (59). As mentioned above, applications of scFv include neutralization, imaging and site-directed drug delivery. There have been successful cases where scFv's are successfully deployed for targeting arthritic cartilage (70). Moreover, scFv has a valuable role in cancer therapy and imaging. While both scFv and IgG can be radiolabeled for tumour imaging and therapy and are used to evaluate pharmacokinetics of the antibody therapeutics, IgG is not ideal for delivering radionuclides because of its large molecular weight (61). Such characteristics make IgG very slow to penetrate tumours while the majority of the non-penetrated labeled antibodies are present in the plasma, this result in poor contrast and exposure of normal tissue to radiation (61). Scfv, particularly its dimer, provides the best balance between penetration and retention half-life (61).

All of these fragments can now be screened and expressed in vitro using library-screening technology such as phage display, which will be discussed below (59). This allows a cost-effective and non-labour intensive method to

rapidly produce monoclonal antibody with specific antigen binding affinity. Although these antibody fragments allow a more convenient way to screen and express fully human antibody, their short in vivo half-life is the major disadvantage of these fragments (59). In the case of Fabs and dAbs, plasma half-life can be prolonged by simple conjugation such as PEGylation (59). However, in the case of scFv's, almost all amino acids of the fragment are critical to the folding of protein and binding to antigen, PEGylation usually will result in a significant drop in binding efficiency (71). While there are still successful cases of PEGylation of scFv's (61), such method should be used cautiously (71). On the contrary, due to the small molecular weight, modifications for peptide drug such as peptidomimetics may become more suitable for enhancing the stability of these fragments (71, 72).

## **1.6. Phage Display**

Phage display is an in vitro high throughput screening technique first described in 1985 by G.P. Smith (73). It is especially useful to generate valuable information on protein-ligand interaction, therapeutics peptide screening, and antibody screening (74-83).

The main component of this in vitro technique, the M13 filamentous phage, has the same property as all other bacteriophages in that these phages are viruses capable of infecting various Gram-negative bacteria which use pili as receptors (74, 76, 84, 85). It contains 11 genes and is 63Å in diameter and 9300Å in length (84). In addition to this basic property, the M13 filamentous phage has

the unique characteristic of being able to trigger the infected *E.coli* into a state of producing and secreting phage particles without undergoing cell lysis (74, 84). The M13 filamentous phage contains a single-stranded DNA as its genetic material, encapsulated by several different coat proteins. Each M13 phage is coated with 2700 proteins encoded by gene VIII, or pVIII as the major capsid coat and capped with 2 minor coat proteins on each end - pIII and pVI on one end, pVII and pIX on the other (74, 76, 84, 85).

The M13 filamentous phage initiates its life cycle by first infecting *E.coli* (e.g. *E.coli* TG1 used in this study) by attaching the pIII to the bacterium's pilus (74, 85). Once the attachment is successful, the single stranded DNA from the phage is inserted into the bacterium and starts to accumulate (84). At this point, the DNA replication machinery is "hijacked" to convert the single-stranded phage DNA into double-stranded replicative form (74, 84, 85). The replicative form then either continues to hijack the host DNA replication machinery to produce single-stranded DNA by rolling circle replication or acts as a template for expressing phage coat proteins (74, 84, 85). Daughter phages are then made by packaging the single-stranded template DNA into the necessary coat proteins and secreted out of the bacterial host into the medium (74, 84, 85).

The M13 filamentous phage used in phage display has almost identical replication mechanism as its wild-type counterpart, except for the fact that it cannot be replicated on its own. For the M13 filamentous phage in phage display, the single-stranded DNA within the virus does not contain the entire phage genome, but only single-stranded hybrid genetic material, called a phagemid,

containing only a target fragment and a coating protein (73, 74, 84, 85). The phagemid is a cloning vector that contains the replication origins of both M13 phage and *E.coli*, an antibiotic resistant gene, and a multiple cloning site for sub-cloning the desired insert (73, 74, 83-85). These phagemid-containing clones can only replicate the single-stranded DNA as typical plasmid, but cannot package into a functional phage without the presence of a “helper phage” (73, 74, 84-86). Helper phages are genetically engineered phage particle with a slightly defective replication origin and a truncated pIII gene, but containing all necessary genetic materials for phage replication and production (73, 74, 84-86).

Upon successful infection of the helper phage to a phagemid-containing *E.coli*, the helper phage supplies all required proteins for phage packaging, thus allowing “phage rescue” (73, 74). During the phage packaging process, two possible phages can be generated – Phage containing the truncated pIII derived from the helper phage; or phage containing fusion coating protein provided by the phagemid (73, 74, 86). Depending on numerous factors such as type of phagemid, growth conditions, nature of polypeptide fused to the coating protein and susceptibility of the fusion protein to proteolytic cleavage, the ratio of fusion protein to wild-type can be from 1:9 to 1:1000 (74). However, since phages containing the truncated pIII cannot infect *E.coli* and propagate themselves, only the fusion protein-containing phage will be carried over for amplification and subsequent selection (84, 85). Other than the use of truncated pIII, another approach is to incorporate a trypsin digestion site on the helper phage encoded

pIII so that the non-peptide containing phage can be screened by trypsin digestion (84).

Since there are 5 different coating proteins on a filamentous phage (pVII, pIX, pVIII, pVI and pIII), there are logically 5 different kinds of phage library, each creating fusion to a particular coating protein (75, 84, 87). The phagemid is constructed such that the scFv DNA and the phage coating protein DNA are in tandem but separated by an amber stop codon TAG. When phage is being packaged in non-amber suppressor strain such as TG1, the *E.coli* will translate the amber stop codon into a glutamine residue, in turn synthesizing a scFv-fusion protein. During expression phase, phagemid will be infected into an amber-suppressing strain HB2151, where the translation will halt at the amber codon and generate phage-free scFv. The most common peptide libraries utilize fusion of sequences to amino-terminus of pIII or pVIII, with pIII more common for proteins (75, 84, 85, 88). Other reported minor libraries include peptide or protein fusion to the amino-terminus of pVII and pIX and carboxy terminus of pVI, an artificial pVIII and pIII (73, 75, 83-85, 89). Different phage display systems have their own advantages and disadvantages. Generally, the pVIII phage display system is not favored because it is the major coating protein of the filamentous phage. As the protein-pVIII fusion is expressed and packaged, approximately 2700 copies of the protein will be displayed on the surface of the phage (75, 84, 90). This significantly lowers the size limit of the protein that can be displayed without interfering with the phage packaging process (84). Moreover, the high abundance of protein displaying on the phage surface also present a problem of “avidity”,

where distinguishing low- and high-affinity binders is becoming very difficult (84). Due to the two constrictions, the pVIII system is mostly reserved for displaying small peptides and screening for low affinity binders (75, 84). On the other hand, most phage display libraries, including the Tomlinson I and J libraries used in this study, utilize the pIII fusion system (83). Compared to pVIII, only 3 to 5 copies of pIII are expressed at the tip of a M13 phage. The drastic drop in copy number not only allows fusion of a larger protein, but also eliminates the “avidity” effect in which a high- and low-affinity binders can be distinguished (73, 84). Such library is also backed by research that shows that the amino-terminal fusion of pIII with peptides or proteins does not affect phage packaging and the function of either pIII or the protein of interest (84).

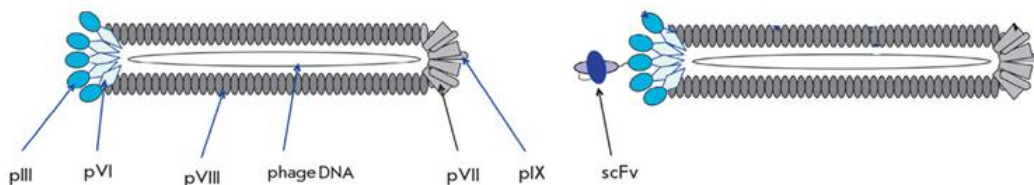


**Figure 1.9 M13 Filamentous Phage and scFv-displaying Phage. M13 filamentous phage is made up of various coating proteins. Fusing scFv DNA with coating protein such as pIII allow native scFv to be displayed on the surface for screening.**

Another important aspect in phage display is the quality and the size of the phage library itself. The term library refers to the collection of *E.coli* with unique phagemid containing the DNA of interest, and encoding either peptides or proteins. It is possible for a library to contain up to  $10^{10}$  unique clones. As the size of the library increases, the probability of isolating an antigen-binding clone and the number of unique antigen-binding clones isolated will also increase. Although more emphasis will be given to the construction of an antibody phage display

library in this review, peptide-, protein- and antibody-library are all fundamentally generated the same way by ligating of site-directed mutagenesis polymerase chain reaction, or PCR, fragments into phagemid vectors followed by *E.coli* transformation (73, 76, 81, 83-85, 87, 90-93). In the case of antibody phage display library, the generation of libraries is accomplished by amplifying the antibody V genes of B lymphocytes from immunized animals using PCR (85). The exact fragment being cloned into the vector system depends entirely on the type of library, such as scFv, dAb, or Fab, wished to be constructed. For the generation of a scFv library, the variable heavy chain and variable light chain gene are amplified and cloned separately into a phagemid vector by ligation(74, 78, 92, 94-96). These libraries can be constructed with or without prior immunization to a particular antigen. If the animal of which the B lymphocytes are purified from is previously immunized with the desired antigen, subsequent panning may yield antibodies that contain even higher binding affinity than from hybridomas (85, 97). Generation of a library from a non-immunized subject is known as a “naïve” library, where heavy and light chains are amplified, randomly combined and cloned into the phagemid construct (85). In some cases, heavy and light chain segments are artificially assembled in vitro. Such library is termed a “synthetic library” (85). The size of a phage library depends on the quality and quantity of source DNA, as well as transformation efficiency (74, 84, 85). A typical antibody library has a size of  $\sim 10^8$  clones with rare libraries containing up to  $\sim 10^{10}$  clones using modified library construction strategies (74).

The principle of a phage display involves repeated screening of peptide-, protein- or antibody-displaying phages and subsequent phage rescue and propagation. The process first starts by incubating the phage library with the antigen, either immobilized, in solution, or on cell surface (74). Subsequently, unbound phages are washed away and antigen-bound phages are retained. The bound phages are then eluted by either trypsin or pH change. These enriched phages are then used to infect *E.coli*, where they will be amplified and propagated (74, 84). This process is termed “panning” (Figure 1.1). Despite the fact that theoretically one round of panning is sufficient to isolate desired phage clone, multiple rounds (between 2-4) are needed in reality to assure high antigen binders are isolated (74). After several rounds of panning, the enriched positive phages are used to infect a different strain of *E.coli*, where the phage-free soluble form of peptides, proteins or antibodies is expressed. In the case of phage display using an antibody phage library, the process of panning for an antigen-binding antibody mimics the biological process of antibody maturation (74, 84, 85, 93, 98). While generating antibody through immunizing an animal and subsequent hybridoma screening is a costly and labour intensive process, phage display provides a rapid, yet cost effective mean of generating specific antigen-binding antibody (84, 98). Due to this reason, phage display has become increasingly popular for antibody screening (84).

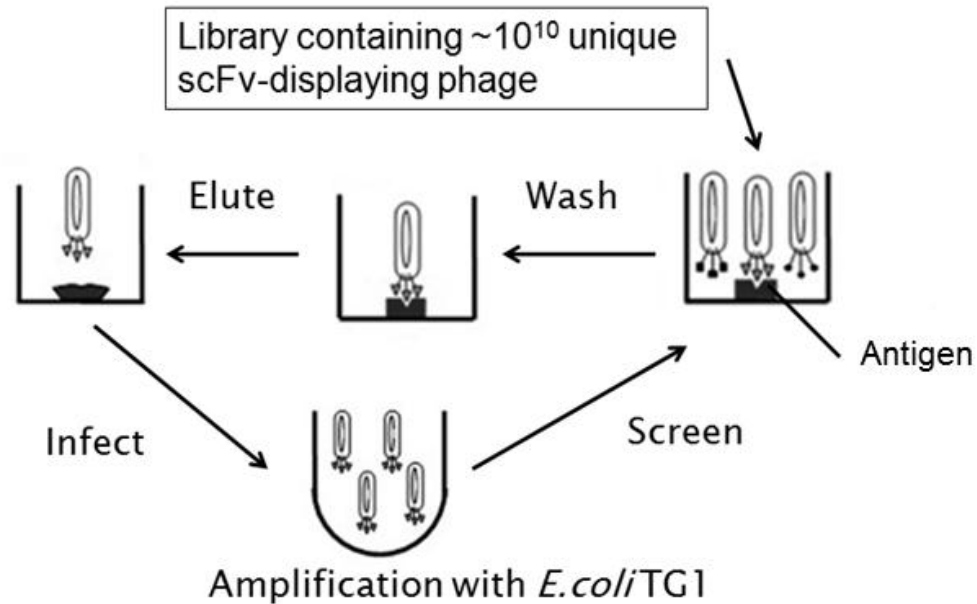


**Figure 1.10 Overall Concept of Phage Display.** Antigen is first coated into wells, which are then incubated with scFv-phage for binding. Unbound phages are washed while the bound phages are subsequently eluted and amplified in *E. coli*. It is common to screen the amplified phage a couple times more to ensure positive clones are identified.

With the versatility of creating different types of library for phage display, the applications of phage display can be classified into two main categories: in vitro diagnostics and in vivo therapeutics (74, 84, 96). In a synthetic oligonucleotide library generating random peptides, its highly randomized nature allows the identification of peptides with binding affinity to a variety of antigens such as antibodies, protein receptors or even endogenous proteins (74). In many cases, phage display of peptides is useful for identifying sequence motifs necessary for binding between two proteins, such as ligand-receptor binding (74, 82, 99). There is even literature reporting that such libraries were used for mapping antibody epitopes (74). These “affinity reagents” not only can serve as therapeutics where site-directed drug delivery is made possible, but they can also become potent inhibitors as these screened peptides may block an enzymatic

active site, or prevent an endogenous ligand binding to its receptor (75, 77, 84, 89). Such applications are especially useful in cancer therapy as cancerous cells often express a characteristic surface receptors, where phage display of an antibody library can generate cancer cell-binding antibodies to be used as a drug-delivering vehicle or potent inhibitors (80, 82, 93, 100). There is literature citing positive result with displaying enzymes on phage (74). Enzymes such as alkaline phosphatase,  $\beta$ -lactamase and trypsin have all been successfully displayed on phage to try to improve their stability and enzymatic activity (74). In addition to the above mentioned general applications of phage display around protein-protein interactions, phage display also has its application in studying peptide sequences to improve protein stability, designing vaccines, analyzing mutant affinities, creating artificial transcription factors and even identifying protease substrates (79, 84, 96). Despite being a technique that is close to 30 years old, phage display is a technique that is still expanding (84, 101). Combining the advances in biotechnology with the creativity of scientists, it is certain that phage display has yet to reach its full potential and undoubtedly there will be many more applications discovered.

## **2. Overview and Hypothesis**

Osteoporosis is a serious disease, especially in elderly women, that is creating an increasing financial burden on the healthcare system. Although there are multiple successful antiresorptive treatment options in the market today, many of these treatments have disadvantages such as poor bioavailability and significant side effects.

With the emergence of antibody therapeutics and the success of Denosumab in osteoporosis treatment, antibody-based treatment has proven to have the potential of becoming a new class of antiresorptive therapeutics. Moreover, with the increasing knowledge of bone turnover markers, antibodies can also be utilized as diagnostic tools for monitoring disease progression, effectiveness of treatment and even patient compliance with therapies for osteoporotic patients.

While most monoclonal antibodies are generated using animal immunization, a cost-effective, time efficient and non labour intensive in vitro antibody screening technique has emerged recently. This technique, known as phage display, is a high throughput in vitro library-based screening platform that allows isolation of antigen-specific scFv within 4-6 weeks. Using this technique, we sought to generate osteoclast-targeting human scFv that could be evaluated as candidates in part of the larger universal bone-targeting platform program in Dr. Doschak's research group. Unlike Denosumab, the purpose of the scFv is simply to generate a drug-carrying vehicle that can deliver low bioavailability drugs such as calcitonin and cathepsin K inhibitor to the site of action on bone tissue for

increased potency. Moreover, with the lack of progress in the diagnostic aspect of osteoporosis, we would like to generate various bone-turnover marker-binding scFv's in order to develop an immunoassay, which is the first step in our end goal of creating a point-of-care patient test kit for evaluating treatment effectiveness and patient compliance.

Recently, there have been reports in the literatures that various osteoporosis therapeutics, particularly calcitonin and 2<sup>nd</sup> generation bisphosphonate, are also effective in treating bone modifying diseases such as osteoarthritis (102-104). These therapeutic options are found to play a significant role in inhibiting subchondral bone remodeling during early phases of osteoarthritis. As such, targeting osteoclasts and regulating subchondral bone remodeling could play a critical role in the pathogenesis of early osteoarthritis (105-107)

Therefore, our objective is: **To generate, without the immunization of mice, osteoclast surface receptor and bone turnover marker-binding molecules for bone targeted drug delivery and for use in diagnostic assays against osteoporosis and potential cross application in disease such as osteoarthritis.** In order to complete our objective, we have outlined two general hypotheses and three specific aims.

Hypothesis: Osteoclast surface receptor and bone turnover marker-specific scFv's can be generated using in vitro phage display and employed as drug delivery vehicles and can be used as alternatives to conventional antibodies in the development of immunodiagnostic assays.

*Specific Aim #1:* To generate anti-RANK scFv for bone targeted drug delivery.

While scFv against various antigens have been isolated by phage display, there has been no literature reported on the isolation of any bone-targeting scFv. We will be using a commercial library, the Tomlinson I + J Human Single Fold Phage Library from Dr. Greg Winter's Lab, purchased from Source Bioscience UK, to carry out the selection procedure. Once isolated and purified, the scFv will be characterized and tested using techniques such as DNA sequencing, ELISA, and western blot.

*Specific Aim #2:* To generate bone turnover marker-specific scFv's, anti-osteocalcin and anti-CTX, for used as potential osteoporosis diagnostic reagents.

We will be using the same library and technique to isolate anti-osteocalcin and anti-CTX scFv. While many commercial biomarker immunoassay kits are available in the market, many of these utilize IgG monoclonal antibody generated from animal immunization. We wish to evaluate a cost-effective way to generate an antibody that is comparable to these kits.

*Specific Aim #3:* To develop a bone-turnover marker immunoassay using generated anti-osteocalcin and anti-CTX scFv's.

The generated bone turnover-binding scFv will be used to develop an immunoassay with OVX rat serum samples. The assay result will be compared with one generated from using a commercial kit.

## **3. Materials and Methods**

### **3.1. Phage Display**

The phage display library used in this entire thesis was the Tomlinson I + J Human Single Fold scFv Library purchased from Source BioScience, UK. In our study, only the Tomlinson I library was amplified because we initially predicted that more than 3 different scFv's would be identified for each antigen, which would be a sufficient number since a large number of scFv's would require additional selection in order to select the best candidates for further study.

The libraries were constructed in the pIT2 construct, which contained both myc and 6xHis tag. These semi-synthetic libraries incorporated randomized codons at 18 sites within the scFv DNA, of which 11 were at the heavy chain and 7 were at the light chain. The Tomlinson I library was estimated to contain  $1.47 \times 10^8$  unique scFv's.

#### **3.1.1. Helper Phage Production**

Before the phage display screening process can commence, it is necessary to produce the KM13 helper phage that is required for initial production and for phage propagation after every round of antigen screening. To produce KM13 helper phage, a single colony of *E.coli TGI* (provided along with the purchase of the Tomlinson I + J library) was inoculated into 2mL of 2xYT medium, which composed of 16g Tryptone (BD, NJ USA), 10g Yeast Extract (BD, NJ USA), 5g NaCl (Fisher Chemical, Canada) and pH 7.0 in 1 litre of water, and grew shaking at 37°C and 250RPM until OD<sub>600nm</sub> reached 0.4, at which time 200µL of this

culture was infected with 10 $\mu$ L of the 100-fold serial diluted of the KM13 helper phage (provided along with the purchase of the Tomlinson I + J library) at 37°C for 30 minutes. After infection, the culture was added at 3mL of molten top agar (50°C), which was made with 0.7% Bacto-agar w/v in 2xYT medium, poured onto 37°C pre-warmed YT plate, which was made from 15g Bacto-Agar (BD, NJ USA), 8g NaCl (Fisher Chemical, Canada), 10g Tryptone (BD, NJ USA), 5g Yeast Extract (BD, NJ USA) and 1% Glucose (Sigma Chemical, MO USA), and incubated at 37°C overnight.

In the next morning, a single colony of TG1 was inoculated into 5mL of 2xYT and grew shaking at 37°C and 250 rotations per minute (RPM) until OD<sub>600nm</sub> reached 0.4, at which time a small translucent plaque was added to the culture and continued to grow for about 2 hours at 37°C. The culture was then added to 200mL of 2xYT and grew shaking at 37°C and 250RPM for 1 hour, at which time kanamycin was added to a final concentration of 50 $\mu$ g/mL and grew shaking overnight at 30°C and 250RPM.

Subsequent morning, the overnight culture was pelleted by centrifugation at 3000rcf for 1 hour. The pellet was discarded and 50mL of PEG/NaCl, which consisted of 20% w/v PEG 8000 (Fisher BioReagent, Canada) and 2.5M NaCl (Fisher Chemical, Canada), was added to the supernatant. The mixture was then left on ice for 1.5 hour for phage precipitation. After incubation, the precipitate was pelleted by centrifugation at 3000rcf for 1 hour at 4°C, where the supernatant was discarded and the pellet was resuspended in 40mL of PBS, which composed of 5.84g NaCl (Fisher Chemical, Canada), 4.72g Na<sub>2</sub>HPO<sub>4</sub> (Sigma Chemical, MO

USA), 2.64g NaH<sub>2</sub>PO<sub>4</sub>·2H<sub>2</sub>O (Sigma Chemical, MO USA) and pH 7.2 in 1 litre of water, and mixed with 10mL of PEG/NaCl. The resulting mixture was incubated in ice again for 1 hour, and was pelleted subsequently by centrifugation under the same setting. The supernatant was then discarded and the pellet was resuspended in 20mL of PBS and stored at 4°C

For titrating the helper phage stock, 45µL of the phage solution was mixed with 5µL of trypsin stock solution, which consisted of 10mg/mL trypsin (Sigma Chemical, MO USA) in 50mM Tris-HCl (Sigma Chemical, MO USA) pH 7.4 buffer containing 1mM CaCl<sub>2</sub> (Sigma Chemical, MO USA), and incubated at 37°C for 30 minutes. The trypsin treated phage was then diluted in 1mL of PBS and further serial diluted to 10<sup>-15</sup> range. 100µL of the 10<sup>-10</sup> to 10<sup>-15</sup> diluted phage was added to 1mL of 2xYT containing TG1 with an OD<sub>600nm</sub> of 0.4. The resulting mixture was added to 3mL of molten Top agar, poured onto YT plate and incubated at 37°C overnight. Phage titre was then determined by counting the number of translucent plaque on the dilution plate possessing 100 – 300 visible plaques.

### **3.1.2. Amplification of Phage Library**

The Tomlinson I Human Single Fold scFv library (Source BioScience, UK) aliquot was added to 200mL of 37°C pre-warmed 2xYT containing 100µg/mL ampicillin (Sigma Chemical, MO USA) and 1% glucose. The culture was left to shake at 250RPM at 37°C until OD<sub>600nm</sub> reached 0.4, at which time 150mL of the culture was taken out and grew shaking at 37°C and 250RPM for 2 hours, while the remaining 50mL was used for phage production described in

section 3.1.3. The culture was then pelleted by centrifugation at 3000rcf for 1 hour, where the supernatant was discarded and the pellet was suspended with 6mL of 2xYT. The resuspended culture was mixed with 3mL of 50% glycerol (Fisher Chemical, Canada) and secondary stock was made by distributing into 20x450µL aliquots and stored at -80°C.

### **3.1.3. Phage Production from Original Library**

To produce phage to commence first round of scFv-phage selection, 50mL of the above-mentioned culture was infected with approximately  $10^{12}$  KM13 helper phage at 37°C for 30 minutes. The infected culture was then pelleted by centrifugation at 3000rcf for 30 minutes, where the supernatant was discarded and the pellet was resuspended in 100mL of 2xYT containing 100µg/mL ampicillin, 50µg/mL kanamycin (Sigma Chemical, MO USA) and 0.1% glucose. The resuspended culture was then incubated shaking at 30°C 250RPM overnight.

The next morning, the overnight culture was pelleted by centrifugation at 3000rcf for 1 hour, where the pellet was discarded and the supernatant was mixed with 25mL of PEG/NaCl. The resulting mixture was incubated on ice for 1.5 hour for phage precipitation. The precipitated phage was then pelleted by centrifugation at 3000rcf for 1 hour at 4°C, at which time the supernatant was discarded and the pellet was 4mL of PBS. The phage solution was spun further at 10800rcf for 10 minutes to remove residual cell debris at stored at -80°C.

For titering the library phage stock, 1µL of phage solution was serial diluted in 100µL PBS until  $10^{-13}$  range. Serial diluted phage solutions from range  $10^{-8}$  to  $10^{-13}$  was added individually to 900µL of 2xYT containing TG1 at an

OD<sub>600nm</sub> of 0.4 and incubated at 37°C for 30 minutes for infection. 100µL of each infected solution was plated individually on YT plate containing 100µg/mL ampicillin and incubated overnight at 37°C. Phage titre was then determined by counting the visible colonies on a dilution plate that possessing 100 – 300 visible colonies.

#### **3.1.4. scFv Phage Selection**

For scFv-phage selection against a desired antigen, 5 wells of a Nunc Polysorp assay strip was coated with 100µL of 100µg/mL antigen – sRANK (Peprotech, NJ USA), Osteocalcin fragment 1-49 (Sigma Chemical, MO USA), CTX (custom synthesized at IBD, University of Alberta, Canada) overnight at 4°C.

Wells were washed the next day with 200µL of PBS 3 times, and subsequently blocked with PBS containing 2% w/v Carnation skim milk (MPBS) at room temperature for 2 hours with agitation. Blocking solution was then discarded and washed again 3 times with 200µL PBS. For scFv phage incubation, 250µL phage stock was first diluted 2x with 2% MPBS, then 100µL of the diluted phage solution was added to each well and incubated at room temperature for 2 hours with agitation.

After incubation, the phage solution was discarded and washed multiple times (10 times for 1<sup>st</sup> round, 15 times for 2<sup>nd</sup> round, and 20 times for 3<sup>rd</sup> round) with 200µL of PBS containing 0.1% Tween-20 (PBST). After washing, the antigen-bound scFv phage was eluted by adding 100µL of trypsin solution, which

was diluted 10 times with PBS from the trypsin stock solution, and incubated at room temperature with agitation for 10 minutes.

After phage elution, 250 $\mu$ L of the eluted phage was added to 1.75mL of 2xYT containing TG1 with an OD<sub>600nm</sub> of 0.4 and the mixture was incubated at 37°C for 30 minutes for infection. 100 $\mu$ L of the infected culture was serially diluted 10 times in 2xYT until a range of 10<sup>-3</sup>. The remaining culture was pelleted by centrifugation at 10800rcf for 1 minute, where the supernatant was discarded and the cell pellet was resuspended with 100 $\mu$ L 2xYT. 100 $\mu$ L of all serial dilutions as well as the resuspended culture was plated on separate YT plate containing 100 $\mu$ g/mL ampicillin and incubated at 37°C overnight.

### **3.1.5. Phage Rescue and Propagation of Enriched scFv Phage**

For amplification of the antigen-enriched scFv phage, 50mL of 2xYT containing 100 $\mu$ g/mL ampicillin with 1% glucose was prepared. Approximately 2mL of medium was used to loosen cells on the resuspended culture plate, of which 600 $\mu$ L was mixed with 300 $\mu$ L 50% glycerol and stored at -80°C as cell stock, while the remaining was used to inoculate the 50mL medium. The inoculated medium was let to grow shaking at 37°C and 250RPM for 1.5 – 2 hours, at which time approximately 10<sup>12</sup> KM13 helper phage was added. The culture was left at 37°C for 30 minutes for infection, and subsequently pelleted by centrifugation at 3000rcf for 30 minutes. The supernatant was discarded and the pellet was resuspended in 50mL of 2xYT containing 100 $\mu$ g/mL ampicillin, 50 $\mu$ g/mL kanamycin and 0.1% glucose and grew shaking overnight at 30°C and 250RPM.

The overnight culture was pelleted by centrifugation the next morning at 3000rcf for 1 hour, where the cell pellet was discarded and the supernatant was mixed with 12.5mL of PEG/NaCl. The mixture was left on ice for 1.5 hours for phage precipitation, at which time the precipitated phage was pelleted by centrifugation at 3000rcf for 45 minutes at 4°C. The supernatant was then discarded and the pellet was resuspended with 2mL of PBS. The resuspended phage was further pelleted by centrifugation at 10800rcf for 10 minutes to remove remaining cell debris. 250µL of the freshly prepared phage was used for next round of phage selection, while the remaining phage solution was stored at -20°C.

## **3.2. Post-Screening Analyses**

### **3.2.1. Phage Enzyme-linked Immunosorbent Assay**

Individual colony from various round of selection was picked from the serial dilution plates, streaked onto a gridded YT plate with 100µg/mL ampicillin as stock and then inoculated into individual well of a 96-well tissue culture treated plate containing 100µL 2xYT with 100µg/mL ampicillin and 1% glucose per well. The plate was left to grow shaking overnight at 37°C and 250 RPM.

The next morning, 10µL of overnight culture of each well was used to inoculate a second 96-well tissue culture treated plate containing 200µL 2xYT with 100µg/mL ampicillin and 1% glucose per well. The plate was left to grow shaking at 37°C and 250 RPM for 2 hours, at which time 25µL of 2xYT containing 100µg/mL ampicillin, 1% glucose and approximately  $10^{10}$  KM13 was added to each well and left to incubate shaking at 37°C and 250 RPM for infection. After infection, the plate was spun at 2000 RPM for 10 minutes, where

the supernatant was removed by vacuum. The cell pellet was resuspended in 200 $\mu$ L of 2xYT containing 100 $\mu$ g/mL ampicillin and 50 $\mu$ g/mL kanamycin and left to grow shaking at 37°C overnight. On the same day, coat a 96-well certified high-bind ELISA plate with 100 $\mu$ L of 100 $\mu$ g/mL of antigen per well overnight at 4°C.

The 96-well ELISA plate was washed on the next day 3 times with 200 $\mu$ L of PBS, and blocked with 2% Bovine Serum Albumin (BSA) in PBS for 2 hours at room temperature with agitation. The blocking solution was then discarded and the wells were further washed 3 times with 200 $\mu$ L of PBS. At the same time, the overnight culture plate was pelleted by centrifugation at 2000RPM for 10 minutes at room temperature, and 50 $\mu$ L of the phage-containing supernatant was used for phage ELISA. The supernatant was incubated at room temperature with agitation for 1 hour, at which time the wells were washed 3 times with 200 $\mu$ L of 0.1% PBST. Once the wells were thoroughly washed, 100 $\mu$ L of 1:10000 dilution of anti-M13 HRP (kindly provided by Dr. Suresh's Lab) in PBS was added to each well and left to incubate 1 hour at room temperature with agitation. The wells were then washed 3 times again with 200 $\mu$ L of 0.1% PBST, at which time 100 $\mu$ L of substrate solution 3,3',5,5'-Tetramethylbenzidine, or TMB (Sigma Chemical, MO USA), was added to each well and left to incubate at room temperature for 10 – 15 minutes. After incubation, the plate was read at 650nm by a plate reader (BioTek EL808) and analyzed using the software KC Junior.

After analysis by plate reader, clones with the 10 highest  $Ab_{S_{650nm}}$  readings were picked from the gridded plate and inoculated into 5mL of 2xYT

containing 100µg/mL of ampicillin and left to grow shaking at 37°C and 250RPM overnight, where 3mL of the culture was used for DNA isolation (section 3.2.2), 600µL of the culture was mixed with 300µL of 50% glycerol to stock storage at -80°C and 200µL was used to inoculate medium for phage production to cross infect the expression strain *E.coli* HB2151 (Section 3.3.1).

### **3.2.2. DNA Sequencing**

DNA template from individual antigen-binding clone was isolated using QIAprep Spin Miniprep Kit (Qiagen Sciences, MD USA). 3mL of overnight culture was pelleted by centrifugation at 13000 RPM for 1 minute, with the supernatant discarded and the pellet resuspended in 250µL using the resuspension buffer provided. Subsequently, 250µL of the provided lysis buffer was added to the suspension and mixed by inverting 4-6 times. The mixture was then neutralized by the addition of 350µL of the provided neutralization buffer and mixed by inverting 4-6 times. The resulting mixture was spun with centrifuge at 10800rcf for 10 minute to remove all precipitate. The supernatant was then applied to the provided spin column and spun at 10800rcf for 1 minute to allow binding of DNA to column. 500µL of the provided wash buffer 1 was added to the column and spun for 1 minute at 10800rcf to remove endonucleases, and 750µL of the provided wash buffer 2 was added to the column and spun twice for 1 minute at 10800rcf to remove all salts. Finally, 50µL of the provided elution buffer was added to the column, incubated at room temperature for 1-2 minutes, spun at 10800rcf for 1 minute and collected with a 1.5mL eppendorf tube.

The dye used for DNA sequencing was BigDye v3.1, which was purchased from the MBSU facility at the University of Alberta. 2µL of the BigDye, 3µL of the BigDye buffer, 4µL of the isolated DNA, 1µL of 5µM primer and 10µL DNase and RNase free water were mixed to create a 20µL reaction mixture. The reaction mixture was let to react in a thermocycler for 25 cycles with the following settings: i. Denaturing temperature: 96°C, 30 seconds; Annealing temperature: 50°C, 15 seconds; Extension temperature: 60°C, 2 minutes. All reaction was carried out using primer 5'- CAG GAA ACA GCT ATG AC -3'.

After reaction was completed, 20µL of the reaction mixture was added to 2µL of the provided ethyl-acetate and 80µL 95% ethanol. The resulting mixture was mixed by vortex and incubated on ice for 15 minutes for DNA precipitation. After incubation, the DNA was pelleted by centrifugation at 10800rcf, 4°C for 15 minutes. The supernatant was removed by vacuum and resuspended in 500µL 70% ethanol. The mixture was again mixed by vortex and pelleted by centrifugation at 10800rcf, 4°C for 5 minutes. The supernatant was again removed by vacuum and the dried product was submitted to the MBSU DNA sequencing facility.

The DNA sequence result was obtained as a notepad file via email. The DNA sequence was then analyzed by an online translation tool ExPASy Translate tool (<http://expasy.org/tools/dna.html>)

### **3.3. Production and Characterization of scFv**

The Tomlinson I + J scFv phage display library requires the use of two *E.coli* strains – TG1 and HB2151, where TG1 was used entirely for phage screening and HB2151 was used entirely for scFv expression. TG1 is an amber codon suppressing strain where a glutamine residue will be produced instead of stopping translation when the amber stop codon (TAG) was encountered. This genotype is taken as an advantage where the scFv was fused with the pIII phage protein separated by an amber codon. Therefore, TG1 was used as a phage display strain due to its ability to produce scFv displaying phage. However, as antigen-binding scFv phage clones were identified, the pIII protein was no longer needed. By infecting the non-amber suppressing strain HB2151 with the scFv phagemid, translation would be halted at the amber stop codon and only the soluble antigen-binding scFv will be expressed.

#### **3.3.1. Infection of Positive scFv Phage Clone to *E.coli* HB2151 Expression**

##### **Strain**

Upon the completion of phage ELISA, 200µL from the 10 picked clones overnight culture was used to inoculate 5mL of 2xYT containing 100µg/mL ampicillin individually and the culture was left to grow shaking at 37°C and 250RPM for 2 hours. Subsequently, approximately  $10^{11}$  KM13 helper phage was added to the culture and incubated at 37°C for 30 minutes for infection. Once the infection process was completed, the culture was pelleted by centrifugation at 3000rcf for 30 minutes, where the supernatant was discarded and the pellet was

resuspended in 5mL of 2xYT containing 100µg/mL ampicillin, 50µg/mL kanamycin and 0.1% glucose. The resuspended culture was left to grow shaking at 30°C and 250RPM overnight.

The overnight culture was spun at 3000rcf and 30 minutes in the next morning, where the pellet was discarded and the supernatant was mixed with 1.25mL of PEG/NaCl. The resulting mixture was incubated on ice for 1.5 hours for phage precipitation and subsequently pelleted by spinning at 3000rcf for 45 minutes at 4°C. The supernatant was discarded and the pellet was resuspended in 200µL of PBS. The resuspended phage solution was spun again at 10800rcf for 10 minutes to remove residual cell debris. 100µL of the purified phage solution was used to infect 200µL of 2xYT containing *E.coli* HB2151 with OD<sub>600nm</sub> at 0.4. The mixture was left for infection at 37°C for 30 minutes, at which time 10µL was plated on YT plate containing 100µg/mL ampicillin and 1% glucose. The plates were incubated at 37°C overnight, where the colonies on plates were used for inoculation for large scale scFv expression.

### **3.3.2. Large Scale scFv Expression**

Once phage selection has been completed and antigen-binding clones have been identified and cross infected to the expression strain HB2151, a large scale scFv expression is needed in order to perform further characterization work. A single colony was picked from plate prepared from 3.3.1 and inoculated into 5mL 2xYT containing 100µg/mL ampicillin. The culture was left to grow overnight shaking at 37°C and 250RPM.

2mL of the overnight culture was used to inoculate 250mL of 2xYT containing 100 $\mu$ g/mL ampicillin and left to grow shaking at 37°C and 250RPM until OD<sub>600nm</sub> reached 0.8, at which time Isopropyl  $\beta$ -D-1-thiogalactopyranoside (IPTG) (Fermentas, Thermo Fisher Scientific, Canada) was added to a final concentration of 1mM to induce scFv expression. Once the culture was induced, it was left to shake overnight at 30°C and 250RPM for expression.

### **3.3.3. Purification of Expressed scFv**

After overnight scFv expression, the overnight culture was pelleted by centrifugation at 3000rcf for 1 hour in pre-weighed centrifuge tubes. The supernatant was discarded and the centrifuge tubes were weighed again to determine wet cell pellet weight. The periplasmic fraction of the scFv was extracted by adding 5mL of BugBuster MasterMix extraction buffer (Novagen, EMD Chemicals, NJ USA) for every gram of wet cell pellet. The extraction mixture was incubated on a rotating platform for 1 hour at 4°C to maximize extraction efficiency. In the meantime, 3mL of Ni-NTA slurry, or 1.5mL resin, (Qiagen, MD USA) was washed 3 times with 5mL water at a flow rate of 1.5mL/min.

After extraction with BugBuster MasterMix, the cell debris was pelleted by centrifugation at 19000RPM and 4°C for 25 minutes. The supernatant was then added to the 1.5mL resin and left to incubate on a rotating platform for 2 hours at 4°C for batch binding. After batch binding, the supernatant slurry was loaded onto a Bio-Rad Econo (20mL) plastic column connected in-line with a peristaltic pump to yield a uniform volume flow of 1.5mL/min. The extract was passed through the

column entirely at least once to ensure maximum binding. The fraction collected was labeled as “flow through” and 50 $\mu$ L was set aside for subsequent SDS-PAGE (3.3.4) and Western Blot (3.3.5) analyses.

After all flow through fraction was collected, wash buffer 1, which consisted of 50mM NaH<sub>2</sub>PO<sub>4</sub> (Sigma Chemical, MO USA), 300mM NaCl (Sigma Chemical, MO USA), 10mM Imidazole (Sigma Chemical, MO USA) and pH 8.0, was added to the column until minimal protein was detected using Bradford Assay (Bio-Rad, CA USA). Subsequently, wash buffer 2, which consisted of identical NaH<sub>2</sub>PO<sub>4</sub> and NaCl concentration and pH except with 50mM Imidazole, was added to wash the column until minimal protein was detected using Bradford Assay. 50 $\mu$ L from both wash fractions were set aside for subsequent SDS-PAGE and Western Blot.

For eluting the expressed scFv, the column was loaded with 10mL of elution buffer, which consisted of identical NaH<sub>2</sub>PO<sub>4</sub> and NaCl concentration and pH as the wash buffers except with 250mM Imidazole, and sample was collected in 1.5mL fraction for 4 fractions. Once 4 fractions were collected, the resin was resuspended with the remaining elution buffer and 50 $\mu$ L was sampled for subsequent SDS-PAGE and Western Blot.

Since protein aggregation was observed in elution buffer, the first 2 fractions and the later 2 fractions were pooled into 2 separate 3mL samples and underwent overnight dialysis (MWCO = 14kDa) at 4°C against 2L of PBS with buffer changes after 1 and 3 hours. After dialysis, samples were distributed in

300µL aliquot and stored in -20°C and BCA assay (Thermo Scientific, Canada) was also performed to determine the concentration of the purified scFv.

### **3.3.4. Sodium Dodecylsulfate Polyacrylamide Gel Electrophoresis (SDS-PAGE)**

SDS-PAGE throughout this project was performed using solely 10% SDS-PAGE gel. The resolving gel was first casted by mixing 7.2mL water, 3.7mL 40% Acrylamide/Bis Solution 29:1 (2.3% C) (Bio-Rad, CA USA), 3.8mL of 1.5M Tris (Sigma Chemical, MO USA) pH 8.8, 150µL of 10% SDS (Bio-Rad, CA USA), and 150µL 10% ammonium persulfate, or APS (Bio-Rad, CA USA), and 10µL of N,N,N',N'-tetramethyl-ethane1,2-diamine, or TEMED (Bio-Rad, CA USA). The mixture was enough to make 2 gels and it was dispensed into glass plate (1mm thick) by serological pipet until the meniscus was about 2cm from the top. Isopropanol or isobutanol was added on top of the resolving gel mixture to help speed up the gel polymerization process. The gel was left to polymerize for around 1 hour, at which time the organic solvent layer was rinsed thoroughly with water. The stacking gel, which was made by mixing 3.1mL water, 0.62mL of acrylamide, and 1.14mL of 0.5M Tris pH 6.8, 50µL of 10% SDS, 50µL of 10% APS and 8µL of TEMED, was added on top of the resolving gel to the top of the glass plate. The gel comb was then added and the gel was left for 1 hour to polymerize.

Before loading the samples, they were first mixed with the loading buffer at a 5-to-1 volume ratio. Every 10mL of 6x loading buffer was prepared by mixing 1.2g of SDS, 6mg bromophenol blue (Bio-Rad, CA USA), 4.7mL glycerol

(Fisher Chemical, Canada), 1.2mL 0.5M Tris pH 6.8, 2.1mL water and 0.93g Dithiothreitol (Bio-Rad, CA USA). Generally, 5 $\mu$ L of samples were loaded if the gel was to be stained by Coomassie Blue and 1 $\mu$ L of samples were loaded if the gel was used to be transfer onto nitrocellulose membrane for Western Blot (3.3.5).

After sample loading, the gel was run in SDS Running Buffer, which made from 3g Tris, 15.4g Glycine (Bio-Rad, CA USA) and 1g SDS in 1L water, at 100V for 1 hour or until dye front reached about 1cm from the bottom of gel. For Coomassie staining, the gel was separated from its glass support, soaked in Coomassie Staining solution and incubated for 30 minutes with agitation. The gel was then transferred to destaining solution and left to incubate overnight with agitation for destaining.

Coomassie staining solution composed of 10% v/v glacial acetic acid, 0.006% w/v Coomassie Blue dye (Bio-Rad, CA USA) in water. Destaining solution composed of 10% v/v glacial acetic acid and 25% methanol in water. The destained gel was then visualized and stored digitally using the Alpha Imager gel documentation system.

### **3.3.5. Western Blot**

For more sensitive characterization and identification of scFv, Western Blot was used. First part of the Western Blot involved running a SDS-PAGE, which was described in 3.3.4. Subsequently, the gel was stacked with a 0.2 $\mu$ m nitrocellulose membrane (GE Healthcare, UK) of equal or greater area and flanked by filter papers and filter pads. The “sandwich” was then loaded into the transblot system with transfer buffer, which was made from 3.03g Tris, 14.41

Glycine in 1L water and was run at 90V for 90 minutes, where the protein samples were transferred from the gel to the nitrocellulose membrane.

After completion of the transferring process, the membrane was either blocked with 5% MPBS for either 2 hours at room temperature or overnight at 4°C. After blocking, the membrane was first washed 3 times with 0.1% PBST, then incubated with 1:5000 anti-myc or anti-His HRP (Invitrogen, CA USA) detection antibody at room temperature for 1 hour with agitation. The membrane was then washed 3 times with 0.1% PBST, dried with filter paper and developed chemiluminescent signal by incubating with Western Blotting Reagent (GE Healthcare, UK) at room temperature for 5 minutes.

After incubating with the blotting reagent, the membrane was dried, wrapped in plastic wrap and placed within a light seal cassette (Kodak, NY USA). Blotting film (GE Healthcare, UK) was then developed with various exposure times using the developing and fixing solution (Kodak, NY USA) in a dark room. The dot blot, which is a simplified version of a Western blot, was done by first spotting antigen directly onto the nitrocellulose membrane with a 10µL pipet tip, followed by incubation with the primary scFv antibody, then incubated with the detection anti-myc or anti-His HRP antibody. The procedure of developing blotting films for a dot blot was identical to that of a Western blot.

### **3.3.6. Enzyme-linked Immunosorbent Assay**

The certified high-binding assay plate was coated with 100µL/well of 100ug/mL of antigen overnight at 4°C. The coating solution was then discarded the next morning, washed 3 times with 200µL of PBS and subsequently blocked

with 200 $\mu$ L/well of 2% BSA in PBS overnight at 4°C. After blocking, the wells were washed 3 times again with 200 $\mu$ L of PBS and incubated with 100 $\mu$ L/well of scFv antibody of desired concentration in 0.1% BSA in PBS at room temperature for 1 hour with agitation. The incubation solution was discarded, wells were washed 3 times with 200 $\mu$ L of 0.1% PBST and then incubated with 100 $\mu$ L of 1:5000 anti-myc detection antibody at room temperature for 1 hour with agitation. The wells were then washed 3 times again with 200 $\mu$ L of 0.1% PBST and incubated with 100 $\mu$ L TMB substrate solution for 15 minutes at room temperature in the dark with agitation, at which time 100 $\mu$ L of 0.18M H<sub>2</sub>SO<sub>4</sub> was either added to each well to quench the reaction or taken for plate reading directly.

Quenched ELISA plate was then read by the Bio-Tek EL808 plate reader at 450nm while unquenched ELISA plate was read at 650nm. Results for both cases were analyzed using the software KC Junior.

### **3.4. Development of Immunoassay**

#### **3.4.1. Antigen-scFv Titration**

From row A to H, each row of the certified high-binding ELISA plate was coated overnight at 4°C with 100 $\mu$ L of antigen with concentrations of 10 $\mu$ g/mL, 1 $\mu$ g/mL, 800ng/mL, 600ng/mL, 400ng/mL, 200ng/mL, 100ng/mL and 50ng/mL. The coating solution was discarded the next morning and wells were washed 3 times with 200 $\mu$ L of PBS and blocked with 2% BSA in PBS at 4°C overnight. After blocking, wells were washed 3 times with 200 $\mu$ L of PBS and from column 1 to 8, each column was incubated with 100 $\mu$ L of scFv antibody with dilutions of

10x, 50x, 100x, 200x, 300x, 400x, 500x and 1000x at room temperature for 1 hour. The incubation solution was then discarded and wells were washed 3 times with 200 $\mu$ L of 0.1% PBST and subsequently incubated with 100 $\mu$ L of anti-myc HRP detection antibody at room temperature for 1 hour. The incubation solution was then discarded and wells were washed 3 times again with 200 $\mu$ L of 0.1% PBST, incubated with 100 $\mu$ L TMB substrate solution at room temperature in the dark for 15 minutes with agitation, then finally quenched by adding 100 $\mu$ L 0.18M H<sub>2</sub>SO<sub>4</sub> solution. Upon quenching, the plate was read by plate reader at 450nm and analyzed by the software KC Junior.

### **3.4.2. Competitive Enzyme-linked Immunosorbent Assay**

The 96-well certified high-binding ELISA plate was coated with 100 $\mu$ L of 400ng/mL osteocalcin solution overnight at 4°C. The coating solution was then discarded the next morning and wells were washed 3 times with 200 $\mu$ L of PBS. Subsequently, wells were blocked with 200 $\mu$ L of 2% BSA in PBS overnight at 4°C. The wells were washed 3 times again with 200 $\mu$ L of PBS the next morning, then incubated with 50 $\mu$ L of the 5x diluted scFv solution with 0.2% BSA in PBS and 50 $\mu$ L of either standards or serum samples. The samples/scFv mixture was left to incubate at room temperature for 1 hour with agitation, at which time the solutions were discarded and washed 3 times with 200 $\mu$ L of 0.1% PBST. The washed wells were then incubated with 100 $\mu$ L of 1:2500 anti-myc HRP detection antibody at room temperature for 1 hour with agitation, at which time the wells were washed 3 times again with 200 $\mu$ L of 0.1% PBST and incubated with 100 $\mu$ L substrate solution TMB in the dark at room temperature for 15 minutes with

agitation. The plate was then quenched with 100 $\mu$ L of 0.18M H<sub>2</sub>SO<sub>4</sub> solution. Upon quenching, the plate was read by plate reader at 450nm and analyzed by the software KC Junior. For comparison with commercial assay kit, Rat-MID Osteocalcin EIA (IDS, UK) was purchased and the protocol was given by the manufacturer.

## **4. Results**

### **4.1. Development of RANK-binding scFv**

#### **4.1.1. Screening of RANK-binding Phage**

The titer of the initial Tomlinson I human single fold scFv library was determined to be approximately  $6.8 \times 10^{13}$  phage/mL. During first round of phage selection for RANK-binding scFv, 250 $\mu$ L, or approximately  $1.7 \times 10^{13}$  phages were used. Phage ELISA was done after 3 rounds of selection to identify positive clones and determine selection efficiency. Figure 4.1 shows the percent of clones identified as RANK-binding positive clones. The screening, or panning, efficiency significantly increased after each round. Figure 4.2 shows a histogram of the sample absorbance readings to demonstrate the bimodal phenomenon observed during phage panning.

Upon successfully picking 10 clones with the highest absorbance readings, which correlates to strong or abundant binders, plasmid DNA for each clone was isolated and DNA sequencing was performed in order to deduce the amino acid sequence of the positive scFv's. Interestingly, while 2 of the 10 clones failed to be sequenced after numerous attempts, the remaining 8 picked clones all possessed identical DNA, and in turn, amino acid sequence. Figure 4.3 shows the deduced amino acid sequence of the RANK-binding scFv.

#### **4.1.2. Purification and Characterization of RANK-binding scFv**

Taking advantage of the 6xHis tag within the scFv-phagemid construct, the desired RANK-binding scFv was purified from the 250mL overnight culture

using the Ni-NTA column. Figure 4.4 shows the SDS-PAGE image of the purification process. While some impurities were found present in the elution fractions, the percentage was deemed lower than 5% judging at the intensity of the desired scFv band in comparison. However, overnight storage at 4°C showed protein aggregation. Therefore, dialysis (MWCO 14kDa) was performed in trying to reduce aggregation. As seen in Figure 4.4, since elution fractions 1 and 2 contained significantly more scFv than elution 3 and 4, the samples were pooled into two separate dialysis tubing (D1 and D2) to prevent unwanted dilution. Figure 4.5 shows the SDS-PAGE image and the Western blot film of the two post-dialysis samples. The two images successfully confirmed the identity of the purified scFv and dialysis has also seemed to reduce protein aggregation significantly. Subsequent BCA assay was performed and the concentrations of D1 and D2 were determined to be approximately 1.6mg/mL and 800µg/mL respectively.

After confirming the identity of the purified RANK-binding scFv, a serial dilution scFv ELISA was performed. Figure 4.6 shows that the binding affinity was in fact retained and its effective working concentration for 1µg RANK antigen is between 16µg/mL and 160µg/mL.

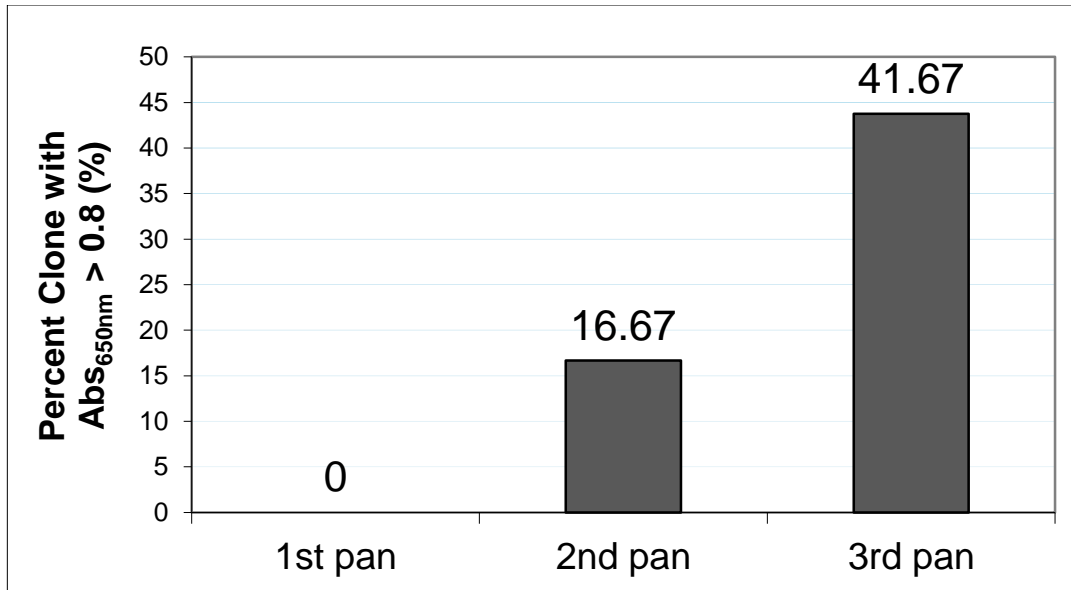


**Figure 4.1: Panning Efficiency of Phage Panning Against RANK.** 92 clones were picked at random from titre plates from all 3 pans. 20, 24 and 48 clones were picked randomly from plates after 1<sup>st</sup>, 2<sup>nd</sup> and 3<sup>rd</sup> round respectively. Percentage of each round was calculated by dividing clones with Abs<sub>650nm</sub> > 0.8 over total number of clones picked for the indicated round.

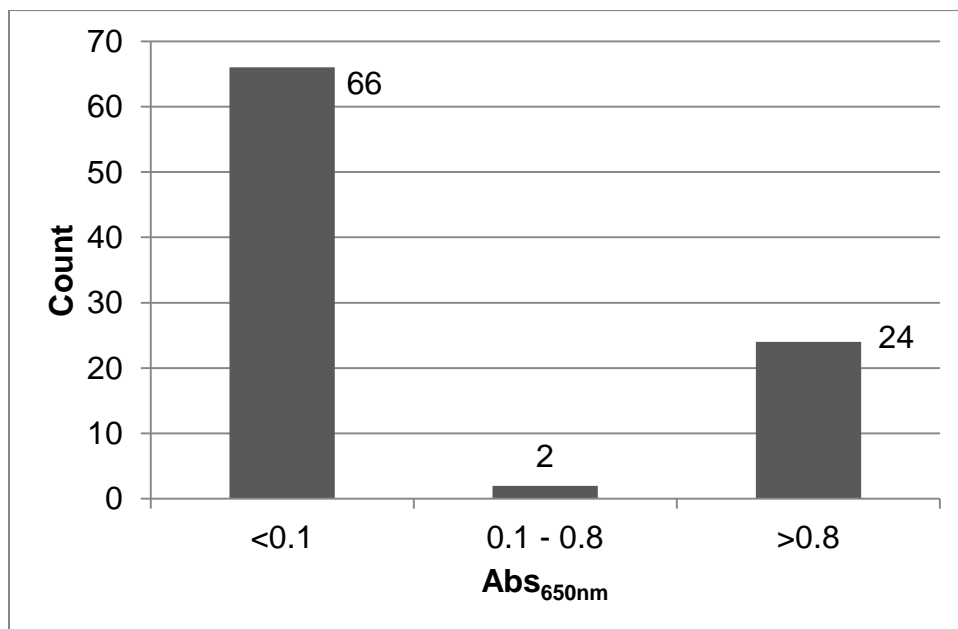


**Figure 4.2 Histogram of Anti-RANK Phage ELISA Abs<sub>650nm</sub> Reading.** Phage clones were classified into non-binder, moderate binder and strong binder base on their absorbance reading. Clones with readings less than 0.1 were regarded as background and thus classified as non-binders. Clones with readings over 0.8 developed intense color after addition of TMB substrate and regarded as strong binders. Clones with readings between the 2 cutoff values were regarded as moderate binders and were not given any consideration for further studies. These colonies correspond to the 92 colonies picked for phage ELISA mentioned in Fig 4.1.

```

MAEVQLLESGGGLVQPGGSLRLSCAASGFTFSSYAMS
WVRQAPGKGLEWVSAISGDGYTADSVKGRFTISR
DNSKNTLYLQNSLRAEDTAVYYCAKNAYSFDYWGGT
LVTVSSGGGGSGGGGGSGGGGGSTDIQMTQSPSSLSASV
GDRVTITCRASQSISSYLNWYQQKPGKAPKLLIYYASSL
QSGVPSRFSGSGSGTDFTLTISSSLQPEDFATYYCQQGS
SSPNTFGQGTKVEIKRAAAHHHHHGAAEQKLISEEDL
NGAA*

```

Figure 4.3 Amino Acid Sequence of RANK-binding scFv. Amino acid sequence of this anti-RANK scFv clone was deduced from obtained DNA sequencing result using primer 5'-CAG GAA ACA GCT ATG AC-3'. DNA sequence was translated to amino acid sequence using an online translation tool ExPASy Translation Tool (<http://expasy.org/tools/dna.html>). Each letter represents the letter abbreviation of individual amino acid sequence. Bolded letters denote the heavy chain of the scFv. Underlined letters denote the light chain of the scFv. Italicized letters denote the poly-glycine serine linker. 6xHis and c-myc tag are highlighted in black. Asterisk (\*) represents translation termination due to the amber (TAG) stop codon.

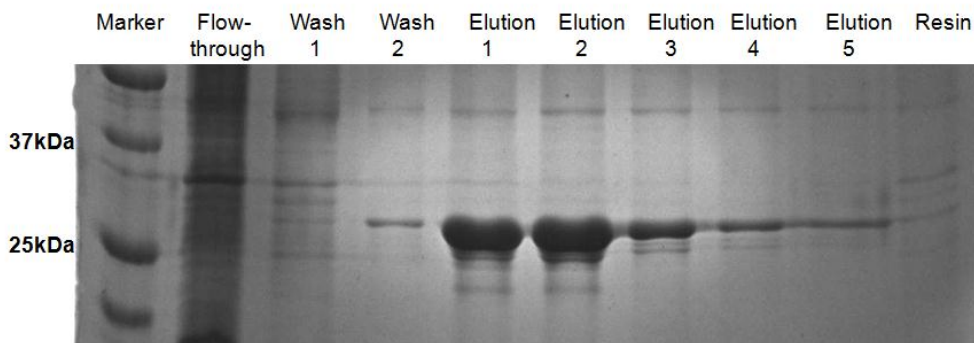
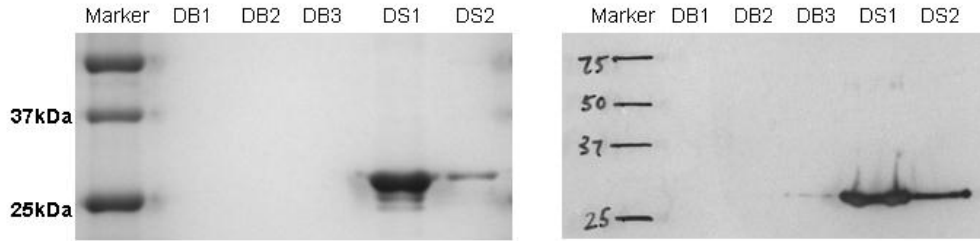
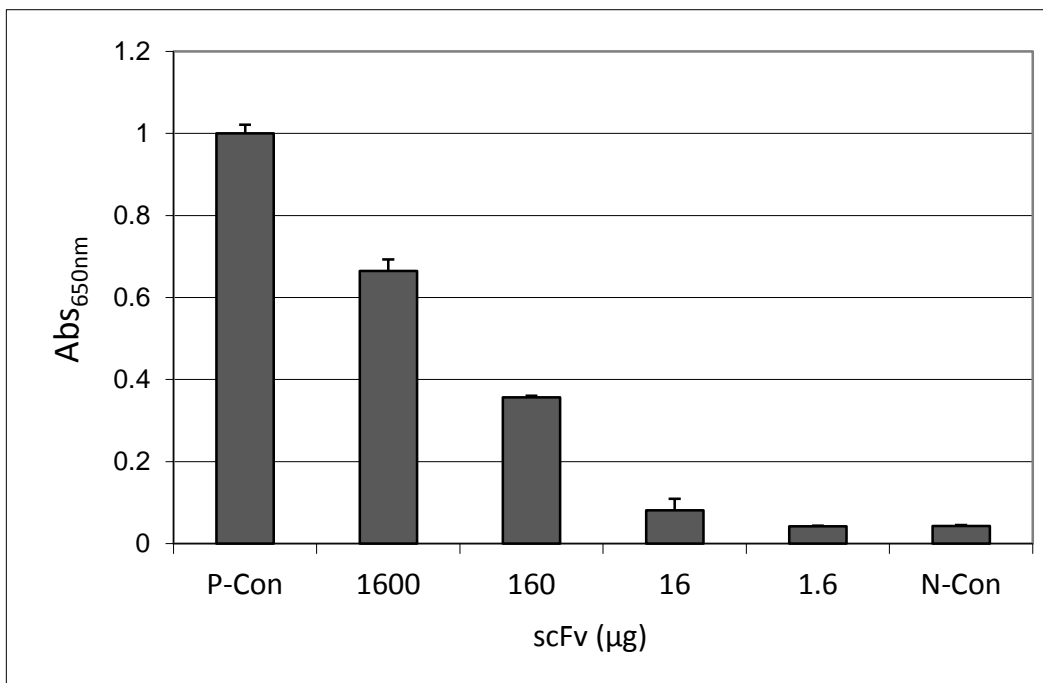


Figure 4.4 SDS-PAGE of Ni-NTA Column Purification of anti-RANK scFv. Each lane was labeled as shown. Purification process was competitive affinity chromatography. Wash 1, wash 2 and elution were performed using Imidazole with concentration 10mM, 50mM and 250mM respectively. 10% SDS gel was used and the gel was run at 100V for approximately 1 hour.



**Figure 4.5 SDS-PAGE (left) and Western Blot (right) Images of dialyzed purified scFv. DB denotes dialysis buffer samples taken during buffer changes while DS denotes dialyzed scFv samples. DS1 was pooled from elution fractions 1 and 2, while DS2 was pooled from elution fractions 3 and 4.**



**Figure 4.6 ELISA of Serial Diluted scFv. Samples were serial diluted  $10$ ,  $10^2$ ,  $10^3$  and  $10^4$  times where the absolute amount is indicated. P-Con denotes positive sample control where wells were coated with undiluted scFv. N-Con denotes negative control where wells were coated with  $100\mu\text{L}$  of 2% BSA in PBS. All other sample wells were coated with  $100\mu\text{L}$  of  $10\mu\text{g}/\text{mL}$  human soluble fraction RANK overnight at  $4^\circ\text{C}$ .**

### 4.1.3. Comparison with Commercial RANK Antibody

After characterization of the purified RANK-binding scFv was completed, it was compared along with commercial monoclonal anti-RANK as well as hybridoma monoclonal anti-RANK generated by my lab colleague Madhuri Newa. Figure 4.7 shows the ELISA reading of the three groups. As expected, given the same amount used, the purified scFv seemed to be outperformed by commercial monoclonal antibody and the hybridoma-generated antibody by 2.5 and 1.8 fold respectively.

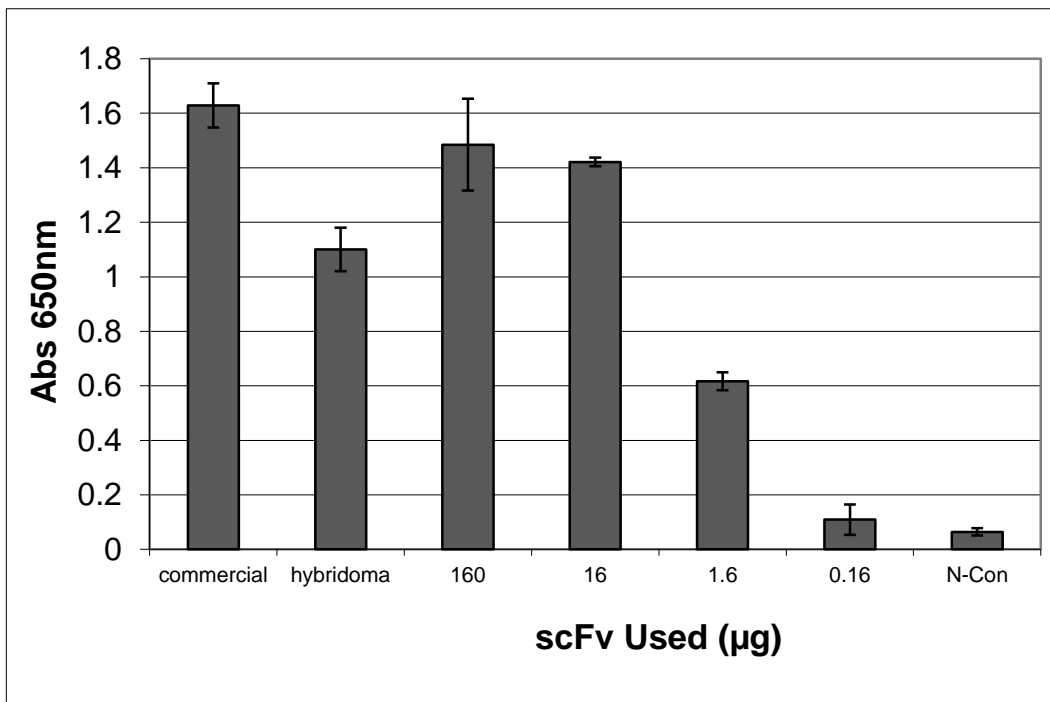


**Figure 4.7 Comparative ELISA of Purified scFv against Commercial and In-lab Generated Hybridoma.** The amount of scFv used during the incubation step was denoted in the horizontal axis. In both commercial monoclonal anti-RANK and in-lab generated monoclonal anti-RANK (synthesized by Ms. Madhuri Newa), 1.6µg was used during the incubation step. N-Con denotes negative control where wells were coated with 100µL of 2% BSA in PBS. All sample wells were coated with 100µL of 100µg/mL human soluble RANK overnight at 4°C. scFv samples and N-Con samples All samples were performed in n=3 except commercial anti-RANK and in-house hybridoma (n=2).

## **4.2. Development of Osteocalcin-binding scFv**

### **4.2.1. Screening of Osteocalcin-binding Phage**

During first round of phage selection for Osteocalcin-binding scFv, 250 $\mu$ L, or approximately  $1.7 \times 10^{13}$  phages were used. Phage ELISA was performed after 3 rounds of selection to identify positive clones and determine selection efficiency. Figure 4.8 shows the percent of clones identified as Osteocalcin-binding positive clones. The screening, or panning, efficiency, although increasing after each round, was much lower than that of phage panning against RANK, with only 20% positive clones after 3 rounds of panning. Interestingly, the bimodal phenomenon that was observed from phage panning against RANK was not present in phage panning against Osteocalcin. Figure 4.9 gives a detailed representation of this observation.

Following the identical procedure as phage panning against RANK, 10 clones that had the highest absorbance readings from phage ELISA was picked for DNA isolation and subsequent DNA sequencing. From the 10 picked clones, 3 unique Osteocalcin-binding scFv's were discovered. Figure 4.10 shows their deduced amino acid sequences.

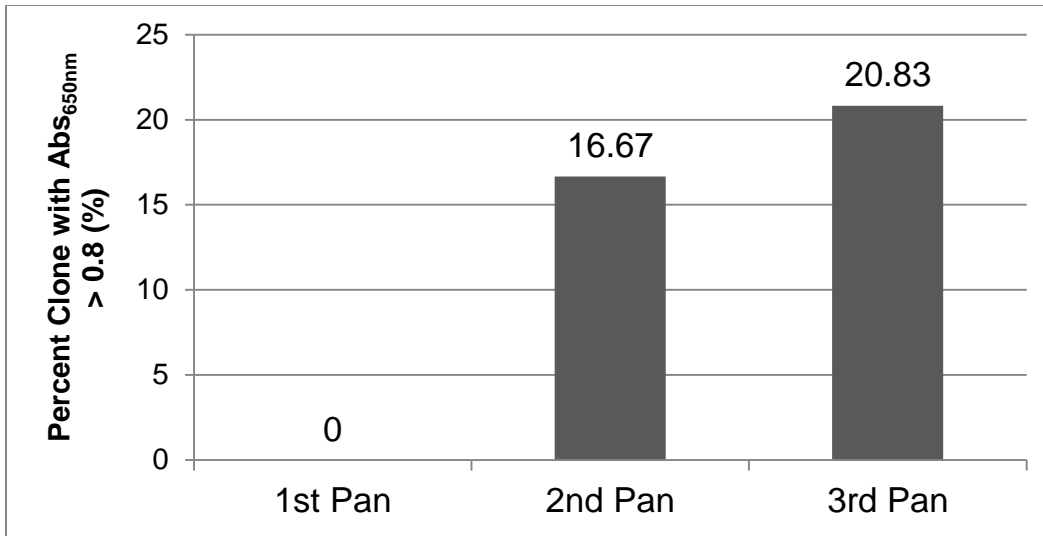


**Figure 4.8 Panning Efficiency of Phage Panning Against Osteocalcin.** 92 clones were picked at random from titre plates from all 3 pans. 20, 24 and 48 clones were picked randomly from plates after 1<sup>st</sup>, 2<sup>nd</sup> and 3<sup>rd</sup> round respectively. Percentage of each round was calculated by dividing clones with Abs<sub>650nm</sub> > 0.5 over total number of clones picked for the indicated round.

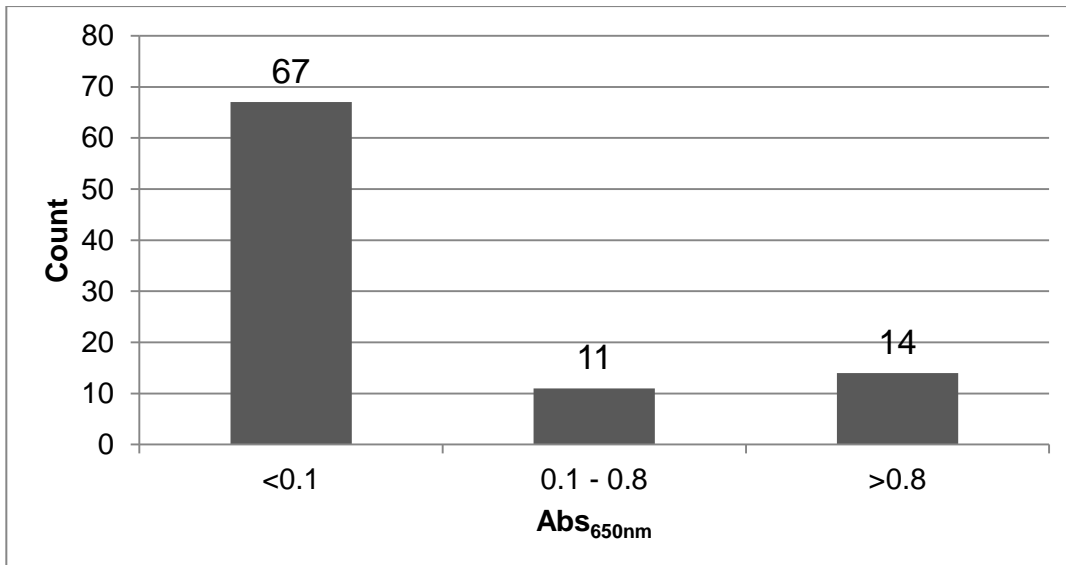


**Figure 4.9 Histogram of Anti-Osteocalcin Phage ELISA Abs<sub>650nm</sub> Reading.** Phage clones were classified into non-binder, moderate binder and strong binder base on their absorbance reading. The cutoff values are identical as the parameters used in the previous pan. Data labels represent the absolute number of clones fall under the indicated category. These colonies correspond to the 92 colonies picked for phage ELISA mentioned in Fig 4.8.

```

OC1 - MAEVQLLES GGGLVQP GGSLRLSCAASGFTFSSYAMSWVRQ
OC2 - MAEVQLLES GGGLVQP GGSLRLSCAASGFTFSSYAMSWVRQ
OC3 - MAEVQLLES GGGLVQP GGSLRLSCAASGFTFSSYAMSWVRQ

OC1 - APGKGLEWVSSIS TGGNAT TYAD SVKGRFTISRDN SKNTLYL
OC2 - APGKGLEWVSSIS SGGSAT SYAD PVKGRFTISRDN SKNTLYL
OC3 - APGKGLEWVSSIT SSGAYT TYAD SVKGRFTISRDN SKNTLYL

OC1 - QMNSLRAEDTAVYYCAK SAYN FDYWGQGTLVTVSSGGGGSG
OC2 - QMNSLRAEDTAVYYCAK SAYT FDYWGQGTLVTVSSGGGGSG
OC3 - QMNSLRAEDTAVYYCAK GSTT FDYWGQGTLVTVSSGGGGSG

OC1 - GGGSGGGG STDIQMTQSPSSLSASVGDRVTITCRASQSISSY
OC2 - GGGSGGGG STDIQMTQSPSSLSASVGDRVTITCRASQSISSY
OC3 - GGGSGGGG STDIQMTQSPSSLSASVGDRVTITCRASQSISSY

OC1 - LNWYQQKPKGKAPKLLIY SASY LQSGVPL LRFSGSGSGTDFTLTIT
OC2 - LNWYQQKPKGKAPKLLIY NASS LQSGVPS SRFSGSGSGTDFTLTIT
OC3 - LNWYQQKPKGKAPKLLIY SASY LQSGVPS SRFSGSGSGTDFTLTIT

OC1 - SSLQPEDFATYYCQQ TAANPT TFGQGTKVEIKRAAA HHHHHH
OC2 - SSLQPEDFATYYCQQ TATNPT TFGQGTKVEIKRAAA HHHHHH
OC3 - SSLQPEDFATYYCQQ SGSSPS TFGQGTKVEIKRAAA HHHHHH

OC1 - GAA EQKLISEEDLN GA *
OC2 - GAA EQKLISEEDLN GA *
OC3 - GAA EQKLISEEDLN GA *

```

**Figure 4.10 Amino Acid Alignment for Osteocalcin-binding scFv's.** OC1, OC2, and OC3 denote the 3 unique anti-Osteocalcin scFv's identified from phage panning. Amino acid sequences were deduced from the DNA sequencing result using the same method as phage panning against RANK. Bolded letters, italicized letters and underlined letters represent amino acids belonging to the heavy chain, poly-glycine serine linker and light chain respectively. 6xHis and c-myc epitope tags were highlighted in black. Asterisk (\*) represent translation termination due to the amber (TAG) stop codon. The unique unconerved amino acid residues between the three scFv clones were highlighted in blue.

#### 4.2.2. Purification and Characterization of Osteocalcin-binding scFv

Using the same procedure for purifying anti-RANK scFv, the desired Osteocalcin-binding scFv's were purified from the 250mL overnight culture using the Ni-NTA column. Figure 4.11 shows the SDS-PAGE image of two dialyzed samples from the 3 purified scFv clones. Interestingly, the expression efficiency of OC3 seemed to be very low and OC2 seemed to have undergone some form of degradation. Western blot (Figure 4.12) confirms the identity of all 3 scFv. From

the inconsistency observed between Figure 4.11 and 4.12, it was suspected that the degradation of OC2 may have been at the C-terminal where the myc-tag may have been degraded. A second Western blot was performed while using anti-His as a detection antibody and further confirmed our speculation (Figure 4.13). Subsequent BCA assay was performed and the concentrations of D1 and D2 of OC1, OC2, and OC3 were determined to be approximately 1.2mg/mL, 300 $\mu$ g/mL, 1.75mg/mL, 440 $\mu$ g/mL, 145 $\mu$ g/mL and minimal respectively. Due to the degradation problem of OC2 and expression problem of OC3, only OC1 was used for further studies.

In order to confirm its retained binding affinity to Osteocalcin, OC1 was used to perform a dot blot. Different amounts of antigen (50ng, 100ng, 120ng, 150ng, 170ng, 200ng) were spotted on the nitrocellulose membrane and incubated with 2 different concentrations of OC1 (60ng/mL and 24ng/mL), followed by detection with 1:2500 anti-myc HRP detection antibody. Figure 4.14 confirms OC1's retained binding affinity.

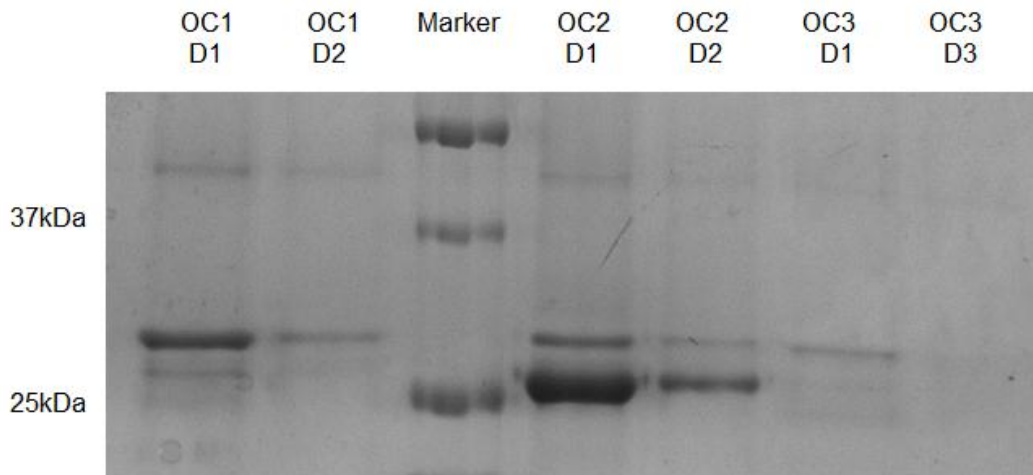


**Figure 4.11 SDS-PAGE of Purified Dialyzed anti-Osteocalcin scFv's.** The 3 unique anti-Osteocalcin scFv's are denoted OC1, OC2 and OC3. D1 and D2 represent the 2 pooled fraction for dialysis where D1 were pooled from elution fractions 1 and 2 while D2 were pooled from elution fractions 3 and 4. 5 $\mu$ L of samples were loaded onto each well. 10% SDS gel was used and it was run at 100V for approximately 1 hour.

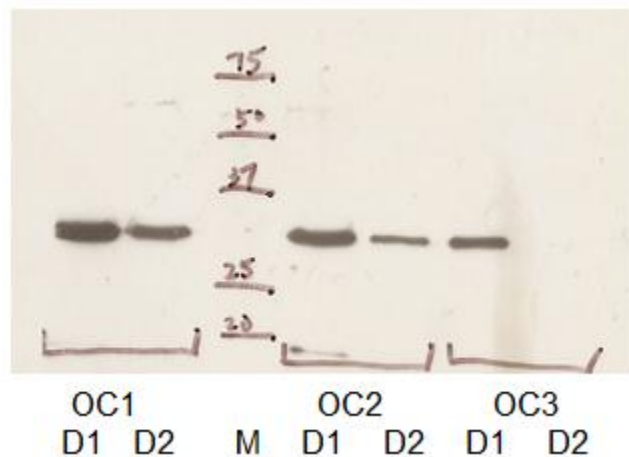


**Figure 4.12 Western Blot of Anti-Osteocalcin scFv's.** 5 $\mu$ L of sample was loaded for each sample well. D1 and D2 represent the dialyzed samples pooled in the same way described in previous images. Transfer was performed at 90V for 90 minutes. Detection was done by incubating 1:5000 anti-myc HRP followed by Western Blotting reagent.

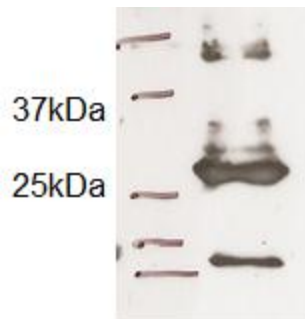


**Figure 4.13 Western Blot of OC2 D1. 5 $\mu$ L of OC2 D1 was loaded. Instead of anti-myc HRP, the sample was detected with 1:5000 anti-His HRP.**

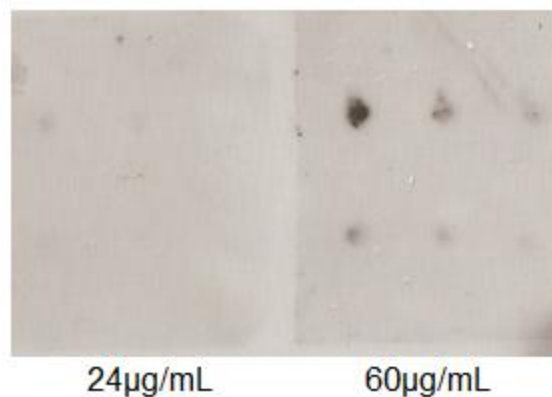


**Figure 4.14 Dot Blot of OC1 Against Osteocalcin. 2 dot blots were performed with 2 different OC1 incubation concentration as indicated. Total of 6 spots were coated on each nitrocellulose membrane. The amounts of osteocalcin spotted, from top left to bottom right, were 200ng, 170ng, 150ng, 120ng, 100ng and 50ng.**

#### **4.2.3. Development of Immunoassay Using Purified Osteocalcin-binding scFv**

The purpose of synthesizing anti-Osteocalcin scFv was to develop an immunoassay for diagnosing osteoporotic patients or evaluating the effectiveness of OP treatment. In order to have a clearer idea of the limitation of the scFv and suitable parameters to use for the immunoassay, a scFv “titration” ELISA was performed. In this ELISA, the plate was viewed as a checkerboard where the coating antigen concentration decreases by rows and the incubating scFv concentration decreases by column. Figure 4.15 shows a relative logical trend of

absorbance readings with slight variation. Since commercial osteocalcin quantitation ELISA kit provides standards between 0 to 120ng/mL and is able to detect in 20 $\mu$ L of serum, more emphasis was given to the part of the graph where a low amount (< 40ng) of osteocalcin was coated in Figure 4.15. Moreover, it can be seen from Figure 4.15 that only scFv with a working dilution of 100X and lower is capable of generating a significant response in absorbance reading. Therefore, the concentration of scFv in attempt to detect Osteocalcin at this range was determined to be around 60 $\mu$ g/mL to 120 $\mu$ g/mL.

Since scFv's can easily be dimerized, sandwich assays cannot be used to directly detect Osteocalcin. Competitive assays are therefore the most logical way to detect Osteocalcin. With the ranges of standards and working dilution for scFv roughly determined, the remaining task was to determine the concentration of the antigen coating solution such that the assay is able to provide significant change in reading with minimal amount of change in osteocalcin. A combination of parameters, such as coating amount, serum sample volume, scFv dilution and volume, and detection antibody dilution, were tested in order generate a significant standard curve within the mentioned range. While increasing the coating amount would decrease the sensitivity of the assay, coating with inadequate amount will lead to weak signals. Different serum sample volumes, scFv dilutions and volumes and detection antibody dilutions were tested in order to find the optimum balance between conservation of reagents and maximizing assay sensitivity. During this optimization process, each parameter was tested individually in order to maximize the understanding of the impact of each

parameter. Figure 4.16 shows the standard curve of a competitive assay which utilized 400ng/mL Osteocalcin coating solution, 50 $\mu$ L of 240 $\mu$ g/mL scFv co-incubated with 50 $\mu$ L of standards and detected by 1:2500 anti-myc HRP, followed by 0.18M H<sub>2</sub>SO<sub>4</sub> quench.

This parameter was used to evaluate serum samples from positive and negative control of ovariectomized rats, which is an established model for osteoporosis, and results were compared with ones obtained from a commercial Osteocalcin quantification kit. As seen in Figure 4.17, a large sampling variability is present. Moreover, possible degradation has occurred in that the absolute Osteocalcin level determined was much lower than what was determined from the commercial kit. In order to solve such issue, a point-to-point ratio value was plotted (Figure 4.18). This will eliminate the sampling variability observed in Figure 4.17 and will also make comparison between scFv and commercial immunoassay possible, since only the trend was being compared. Although the absolute amount determined between assays were different, this may be due to antigen degradation because the assay performed with scFv was done close to 1 year after the assay was performed with the commercial kit.

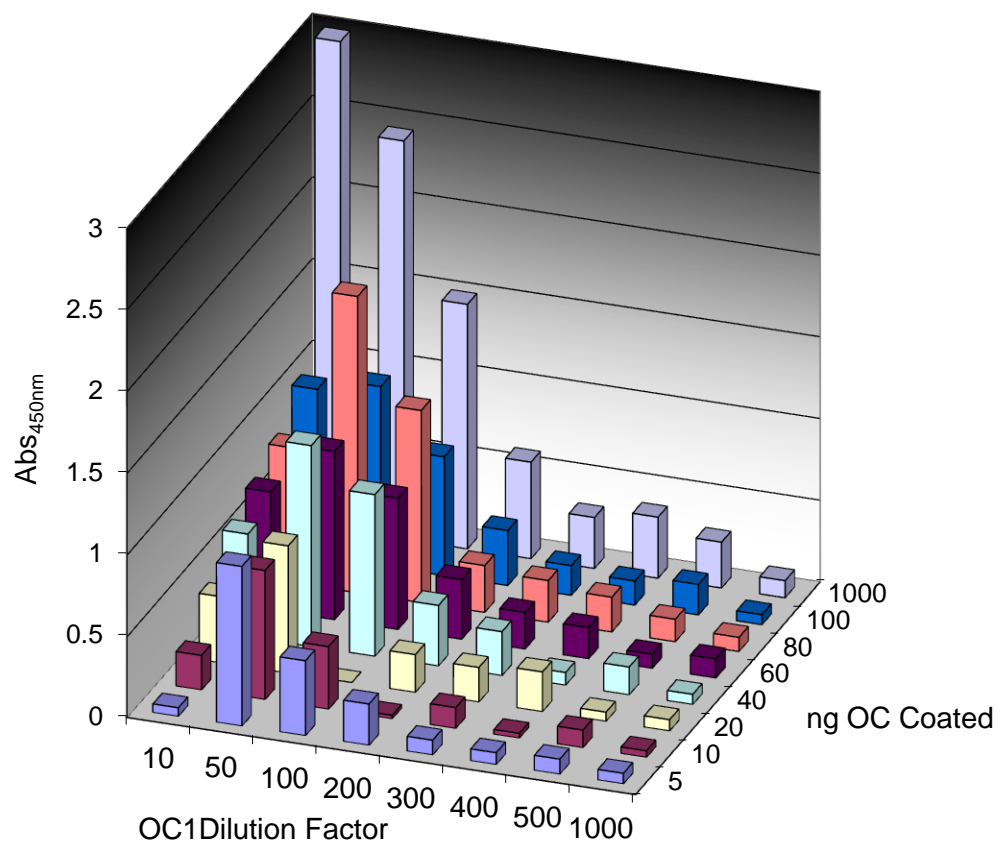


**Figure 4.15 3D Bar Graph of "Checker Board" ELISA Titration using OC1. X-axis represents the dilution factor of OC1 used during incubation step. Y-axis represents the amount of Osteocalcin coated for the ELISA. Z-axis represents the Abs<sub>450nm</sub> readings under the condition denoted by x and y-axes.**

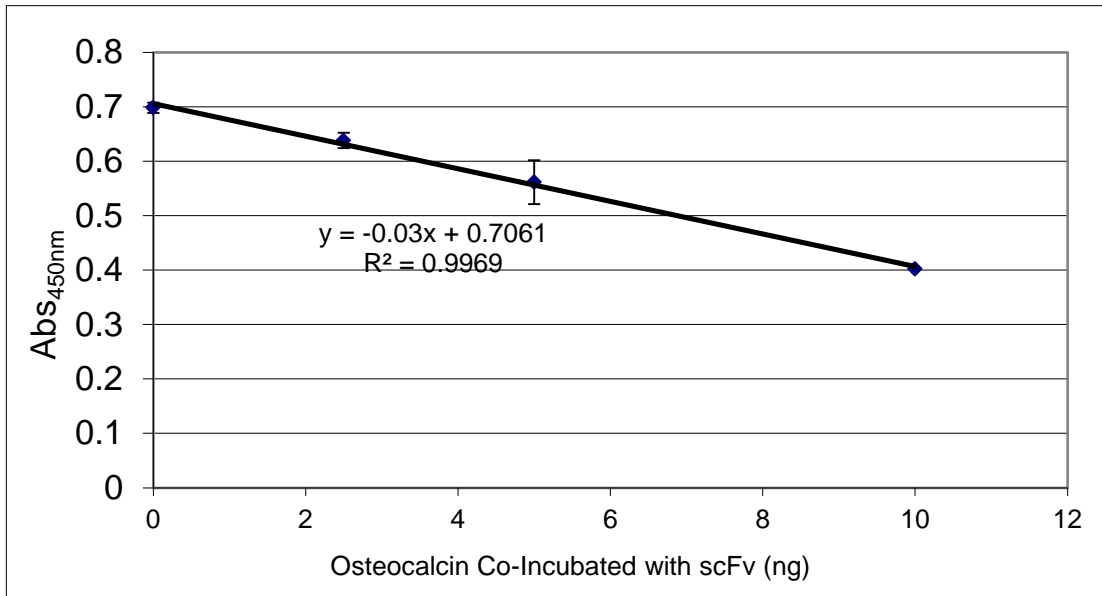


**Figure 4.16 Standard Curve of Osteocalcin Competitive Assay Using OC1 scFv.** The standard curve was generated using 4 standards (n=3) where 50µL of 240µg/mL of OC1 in 0.2% BSA in PBS was co-incubated with 50µL of osteocalcin in PBS with concentration of 200µg/mL, 100µg/mL, 50µg/mL and 0µg/mL. Co-incubation time was 1 hour at room temperature with agitation. 100µL/well of 1:2500 anti-myc HRP was used as detection. 100µL/well of TMB solution was used as substrate, which was quenched by 100µL/well of 0.18M H<sub>2</sub>SO<sub>4</sub>. Each standard was done in triplicate.

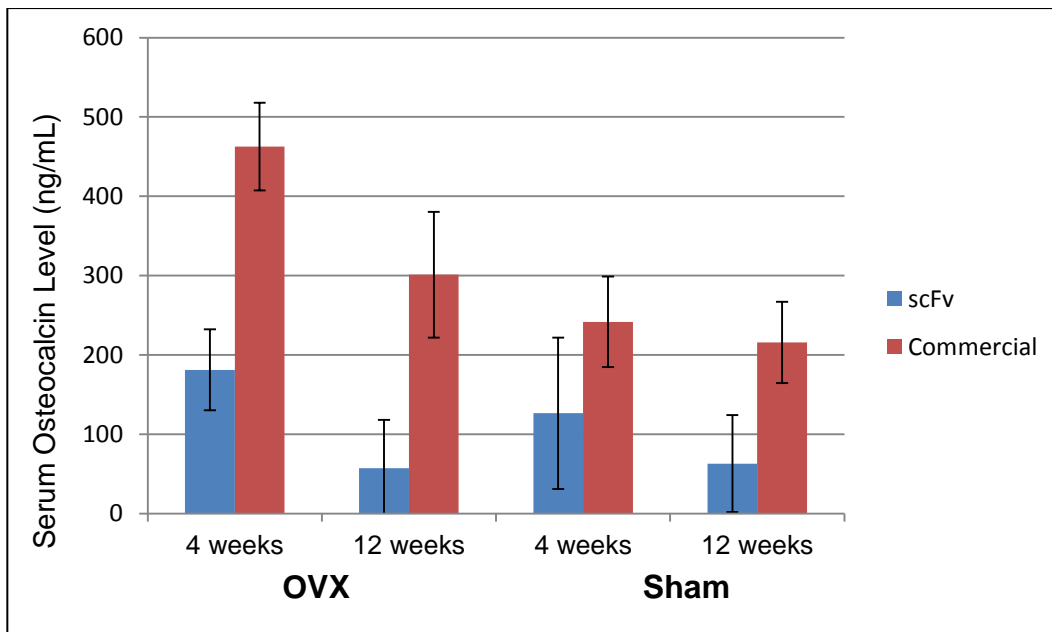


**Figure 4.17 Quantitation of Serum Osteocalcin Using scFv vs Commercial Assay.** Serum of Ovariectomized and Sham rats were sampled at 4 and 12 weeks (n=8). Blue bar denote samples tested with OC1 scFv. Red bar denote samples tested with Commercial Osteocalcin EIA kit purchased from IDS.

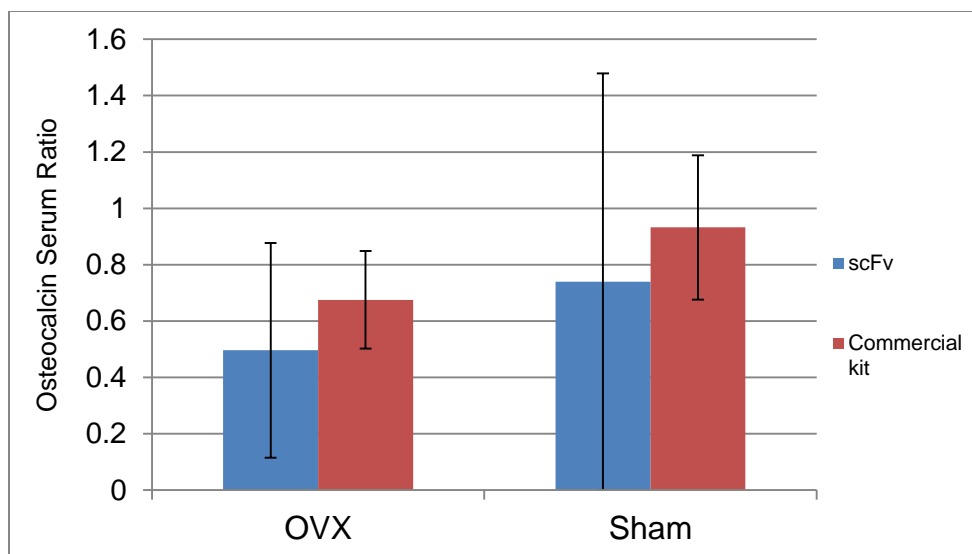


**Figure 4.18 Relative Comparison of Serum Osteocalcin Using scFv vs Commercial Assay.** Serum of Ovariectomized and Sham rats were sampled at 4 and 12 weeks (n=8). Values shown are the ratio of the serum osteocalcin level at 8 weeks to osteocalcin level at 4 weeks. Blue bar denote samples tested with OC1 scFv. Red bar denote samples tested with Commercial Osteocalcin EIA kit purchased from IDS.

### 4.3. Development of CTX-binding scFv

#### 4.3.1. Screening of CTX-binding Phage

Approximately  $3.4 \times 10^{13}$  phages were used in first phage screening attempt for CTX-binding scFv, whereas approximately  $1.7 \times 10^{13}$  phages were used in second and third phage screening attempt. Due to the difficulty of finding a commercial provider of the antigen, a synthetic octapeptide (N-EKSQDGGR-C) was custom-synthesized by the Institute for Biomolecular Design at the University of Alberta. A total of 3 screening attempts were done because although the panning efficiency was high, DNA sequencing revealed that all clones in fact belonged to only 1 unique CTX-binding clone. Furthermore, DNA sequencing showed that this CTX-binding clone contained an amber stop codon in one of the randomized sites in the heavy chain of the scFv DNA construct (Figure 4.21).

Figure 4.19 shows the panning efficiency of the first CTX-phage panning attempt. As mentioned earlier, panning efficiency was similar to the previous phage panning against two different antigens. Figure 4.20 also shows the consistent observation of the bimodal effect found in the phage screening for RANK.

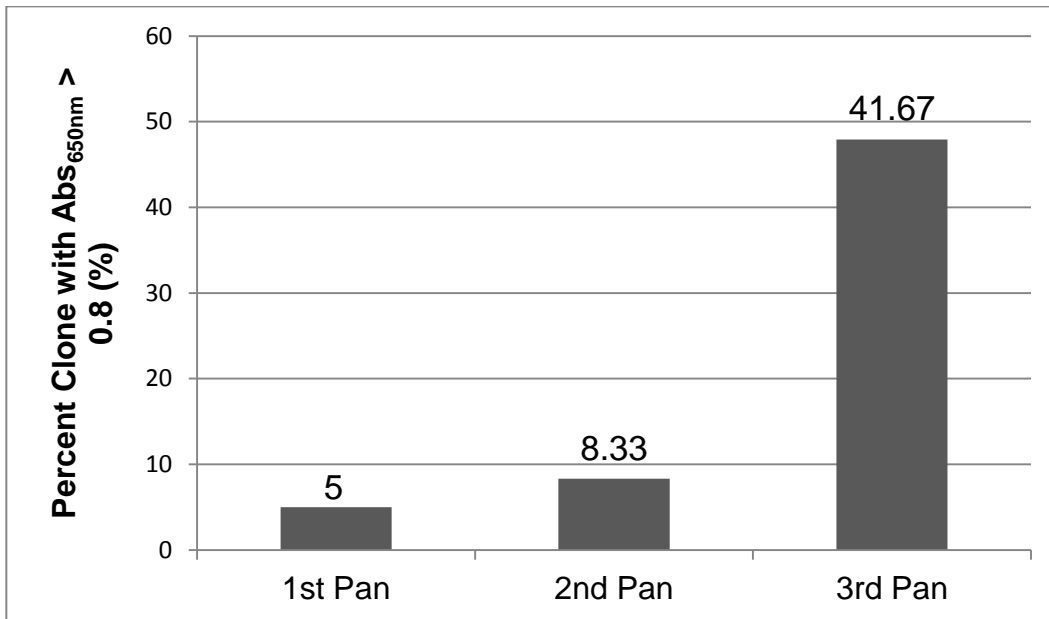


**Figure 4.19 Panning Efficiency of Phage Panning Against CTX.** 92 clones were picked at random from titre plates from all 3 pans. 20, 24 and 48 clones were picked randomly from plates after 1<sup>st</sup>, 2<sup>nd</sup> and 3<sup>rd</sup> round respectively. Percentage of each round was calculated by dividing clones with Abs<sub>650nm</sub> > 0.8 over total number of clones picked for the indicated round.

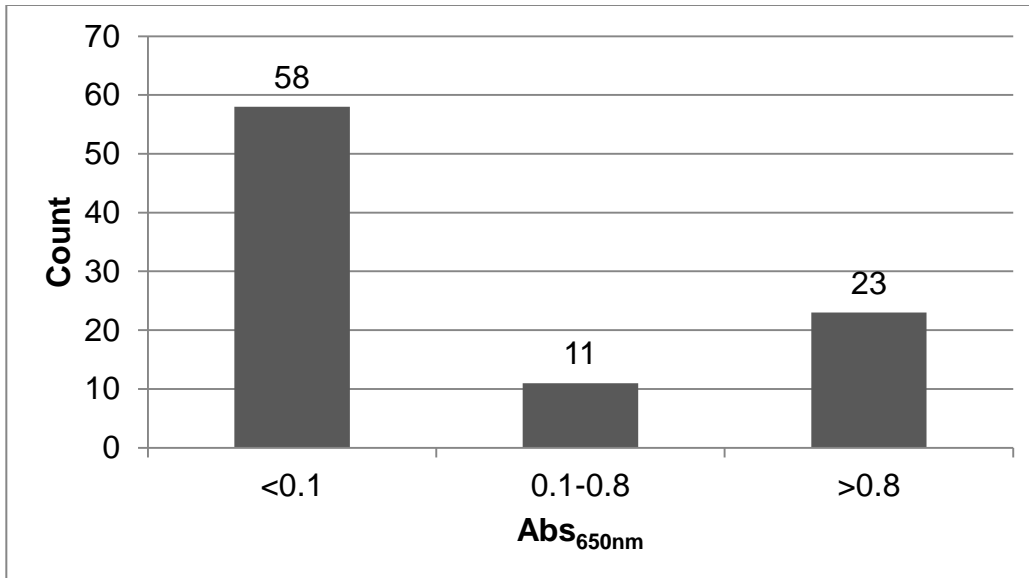


Figure 4.20 Histogram of Anti-CTX Phage ELISA Abs<sub>650nm</sub> Reading. Phage clones were classified into non-binder, moderate binder and strong binder base on their absorbance reading. The cutoff values are identical as the parameters used in the previous two pans. Data labels represent the absolute number of clones fall under the indicated category. These colonies correspond to the 92 colonies picked for phage ELISA mentioned in Fig 4.18.

```

MAEVQLLESGGGLVQPGGSLRLSCAASGFTFSSYAMSWV
RQAPGKGLEWVSSISSTGASTTYADSVKGRFTISRDN SKN
TLYLQMNSLRA*DTAVYYCAKGGAAFDYWGGTLVTVSS
GGGGSGGGGSGGGGSTDIQMTQSPSSLSASVGDRTITC
RASQSISSYLNWYQQKPKAPKLLIYSASYLQSGVPSRFS
GSGSGTDFTLTISSSLQPEDFATYYCQQANNAPTTFGQGTK
VEIKRAAAHHHHHGAAEQKLISEEDLNGAA*

```

Figure 4.21 Amino Acid Sequence of CTX-binding scFv-phage Fusion. Amino acid sequence of this clone was deduced from obtained DNA sequencing result using primer 5'-CAG GAA ACA GCT ATG AC-3'. DNA sequence was analyzed the same method as previous phage screening clones. Bolded letters denote the heavy chain of the scFv. Underlined letters denote the light chain of the scFv. Italicized letters denote the poly-glycine serine linker. 6xHis and c-myc tag are highlighted in black. Asterisks (\*) represent translation termination due to the amber (TAG) stop codon.

## **5. Discussion**

### **5.1. Phage Display and Generation of scFv**

The main goal of this project was to generate molecules that bind specifically and strongly to a particular antigen, so that they can be used in two different applications – as a drug targeting vehicle for therapeutics, or as a bone-turnover marker scavenger for diagnostics. As mentioned in the literature review section, antibodies are a class of molecule that possesses superior binding affinity and selectivity to a particular antigen. These characteristics make antibody a logical choice for our lab to pursue in generating a bone-targeting antibody for therapeutics or a bone-turnover marker antibody for diagnostics.

As the field of biotechnology advances, many modified variations of the conventional IgG antibody have become available for scientists' use. Each of these variations has its own advantages and limitations that were discussed earlier in the previous section. In our study, we have chosen scFv over IgG and other variations for several reasons. Firstly, generation of scFv employs an in vitro method known as phage display, which mimics the affinity maturation of antibody production in a biological immune system. Therefore, it allows us to generate antibodies without animal immunization and subsequent hybridoma culture and screening, which is much more labour intensive and time-consuming. From the initial screening of the original library to obtaining purified and functional scFv's, the entire process takes less than 5 weeks. Moreover, antigen-specific scFv are generated from in vitro screening of an existing scFv-display phage library, which can be used repeatedly for screening against different

antigen, whereas animal sacrifice is necessary for isolating spleen cells for hybridoma culture. In addition, since scFv production is via an *E.coli* bacterial expression system, it is much more cost effective than conventional hybridoma expression, which requires mammalian cell culture. As such, we can take advantage of the closely coupled system between the M13 filamentous phage and *E.coli* as a bioreactor for rapid screening and expression of antigen-binding scFv.

Lack of immunogenicity also gives scFv an advantage over conventional IgG antibody. The scFv-phage library was constructed with the human immunoglobulin gene, which in turn yield scFv recognized as endogenous by the immune system. However, hybridoma antibody was raised from spleen cells of animal such as mice or rabbits. As a result, these antibodies would be recognized as foreign substance by the immune system and would in turn yield an unwanted immune response. Although the xenomouse technology, where the animal's immune system is replaced entirely with the human immune system, yield fully human IgG antibody, the associated cost is higher than the original hybridoma technology, and even more so than phage display.

Lastly, an scFv is a truncated modification of a conventional IgG where everything but the binding domain is completely removed. This significantly reduces the molecular weight of the compound, making it easier to handle. Since an scFv is incorporated into a genetically engineered construct, it also contains artificial epitope tag such as 6xHis and c-myc, which allows easy purification and detection of compound.

However, the main limitation of scFv is its short half-life and subsequent weaker binding affinity. Intact IgG antibody is a large molecule with numerous intramolecular interactions, including multiple chemically covalently-linked disulfide bonds to maintain its structural integrity. ScFv, on the other hand, do not contain any disulfide bonds and possess much fewer intramolecular interactions due to its reduced size. This causes scFv to become more prone to structural changes in solution and much more susceptible to proteolytic cleavage. In order to take full advantage of scFv, a subsequent stabilization step should be in place. With various stabilization strategies reported in the literature and its inherent advantages in cost and labour intensiveness, scFv show potential in becoming an alternative to antibody in site-directed therapeutics and in vitro diagnostics.

## **5.2. Phage Display of RANK-binding scFv**

Our first attempt for developing an antigen-specific scFv using the Tomlinson I library was against human RANK. As mentioned in the literature review section, RANK is a surface receptor that is found on all osteoclasts. By generating RANK-binding molecule, our lab would then be able to use it as a universal osteoclast-targeting platform, which serves as a drug targeting vehicle and carries any conjugated therapeutics to osteoclast to regulate bone resorption rate, thus controlling the progression of osteoporosis.

Using the standard protocol provided by the supplier of the Tomlinson I library with minor adjustments, over 40% of clones show RANK-binding characteristic by the end of 3<sup>rd</sup> round of selection (Figure 4.1). Moreover, phage

ELISA result showed that majority of these randomly picked clones either showed strong binding affinity or no binding affinity (Figure 4.2). As a result, we were confident that the clones chosen for subsequent studies were not false positives. However, we were surprised to realize that all ten picked clones possessed identical DNA sequence (Figure 4.3). This may be due to very stringent washings during the first round of phage screening, where RANK-binding but low abundance scFv phage may have washed away, leaving the RANK-binding and high abundance scFv behind and amplified exponentially over round 2 and 3 of the screening, which contributes to the high percentage of positive clones during phage ELISA. Such a phenomenon was also the reason that only 3 rounds of screening was performed for every antigen – Although increasing the rounds of screening would have lead to higher percentage of positive clones, it also leads a decreasing number of unique clones since the probability of the low abundance antigen-binding scFv phage being washed away also increases. Despite the fact that only 1 unique RANK-binding scFv's was identified, it is sufficient for us to further our studies. Therefore, we did not repeat the screening step and decided to proceed to our subsequent studies with the only clone.

Once the scFv DNA has successfully been transferred to HB2151, a large scale expression was performed and the scFv was extracted and purified by Ni-NTA column chromatography. Figure 4.4 showed that the purification process was relatively successful and large amount of scFv had been purified. Dialysis was later performed in an attempt to improve the protein aggregation problem. It

can be seen from Figure 4.5 that despite minor impurities, a large amount of pure scFv has been isolated.

In order to confirm that the scFv function has been retained after purification and to evaluate the binding affinity of the purified scFv, a serial dilution scFv ELISA was performed. To yield a clearer picture on how scFv compares to its counterparts, a comparison ELISA was also done between scFv, commercial anti-RANK and in-lab generated hybridoma IgG anti-RANK. The result did not surprise us in that the commercial antibody and hybridoma IgG anti-RANK outperformed the scFv by 2.5 and 1.8 fold respectively. Although scFv's contain the necessary domain for antigen binding, they contain only 1 binding domain where as conventional antibodies contain 2 of these domains for increase affinity. Moreover, an IgG antibody is held together by the intramolecular forces and disulfide bonds between its amino acids, whereas an scFv have much of the structural components of an antibody removed and is reduced to its most basic functional part. The removal of a great number of amino acids dramatically decreasing the intramolecular forces that contribute to the structural integrity of an antibody, thus greatly decreasing scFv's structural stability. These limitations are reasons that scFv's are at an inherit disadvantage to convention IgG antibody in terms of binding affinity. However, these limitations can be potentially be overcome by various stabilization strategies, which will be discussed in detail further in the future direction section.

This is the first known successful attempt to isolate any antibody or its analogue that targets bone cells. There have been literatures and clinical trials

reporting antibodies targeting either cartilage or cytokines as treatment for osteoporosis, but the idea of using antibody as a bone-targeting moiety is an area that has yet to be explored. It should be noted that the anti-RANK scFv platform may not be applied only to osteoporosis, for there are reports in literature in the past few years suggesting that osteoclasts also play a significant role in disease such as osteoarthritis (105-107) in the subchondral remodeling phase during early osteoarthritis and targeting such phases may be beneficial in controlling the pathogenesis of osteoarthritis (108, 109). If future studies confirm our preliminary data that anti-RANK scFv is a viable option for site-directed drug delivery, this bone-targeting platform can be useful not only in osteoporosis, but also in osteoarthritis. Moreover, the primary purpose of anti-RANK scFv is to target osteoclast specifically, therefore such technology has the flexibility of chemically tethering various therapeutics for treating different bone modifying diseases by disrupting osteoclast activity with improved bioavailability.

Since bone turnover markers and RANK are both protein-based molecules, our success in generating RANK-binding scFv provided a proof-of-concept that phage display can be used to develop bone-turnover marker-specific scFv. In bone modifying disease such as osteoporosis and osteoarthritis, the balance between bone resorption and bone formation is usually disrupted. By generating scFv's that can scavenge these bone-turnover markers in either patients' serum or urine samples, a quantitative assay, like those that are available commercially for rat serum samples, or even a qualitative point-of-care test kit can be developed for monitoring patient's disease progression, a therapeutics'

effectiveness, or even patient compliance, which could give physicians and pharmacists a powerful tool to aim for the most suitable dosing regimen for their patients.

### **5.3. Phage Display of Osteocalcin-binding scFv**

With the promising result shown from our phage display panning against RANK, we shifted our antigen of interest from cell surface receptor to characteristic bone-turnover marker - Osteocalcin. It is a protein that is released by osteoblast during bone formation. Since bone formation takes place after bone resorption, osteocalcin is considered a late bone-turnover maker. The osteocalcin used for phage panning was slightly smaller than the first antigen, soluble RANK. Therefore, we initially predicted that most likely only 1 Osteocalcin-binding scFv clone would be identified. As seen in Figure 4.8 and 4.9, panning efficiency was significantly lower than that of RANK, with only 20% of the clones showed affinity to Osteocalcin and only 14 clones were considered as strong-binders.

Result shown in Figure 4.10 was a positive surprise for us. A total of 3 unique, non-amber containing Osteocalcin-binding scFv clones were identified. With 3 different clones at our disposal, we had the luxury to choose the most suitable scFv's for expression to further our study in developing an immunoassay for Osteocalcin. Various SDS-PAGE and Western Blot images (Figure 4.11 – 4.13) showed in fact only 1 clone was deemed to be suitable for conducting further studies, where OC3 had very low expression and OC2 appeared to have

undergone degradation. The dot blot (Figure 4.14) confirmed that OC1 has retained its affinity after Ni-NTA purification.

These results demonstrated that as long as the antigens are of an appropriate size, phage display can be used to generate antigen-specific scFv. This is the first known attempt that a scFv showing binding affinity to a bone-turnover marker has been isolated. It should be noted that this technique is not only limited to bone disease, but phage display can also be applied to generate scFv against antigens across all fields – such as toxins, cancer cell receptor, virus and enzymes.

#### **5.4. Immunoassay Development of Osteocalcin-binding scFv**

Our ultimate goal for the application of anti-Osteocalcin scFv is to develop a point-of-care test kit for general physicians and/or pharmacists to test patients for the progression of osteoporosis, the effectiveness of bisphosphonate treatment or even patients compliance with their current treatment. However, with many obstacles such as detection limit and implementation method, the development of an immunoassay was taken as an intermediate step with rats serum samples were used as a pilot study.

In order to obtain a clear idea of the detection limit of scFv, a checkerboard titration ELISA (Figure 4.15) was performed. The goal of this experiment was to locate the right balance between maximal detection and minimum reagent used. Since the detection range of commercial rat serum Osteocalcin ELISA kit is between 0 to 20ng, it was determined that in order to develop a competitive ELISA having a detection limit around such a range, a scFv

working dilution of 10x or less was needed. To optimize the parameter of the assay, a combination of parameters such as amount of antigen coated, volume and working dilution of scFv used, volume of serum co-incubated and volume and working dilution of detection antibody used was tested. While testing each combination, a standard curve was generated and two important characteristics were considered – 1. The linear standard curve possess a negative slope, which is the first indicator that the scFv is sensitive enough to engage in competitive binding between immobilized and soluble antigen; 2. The range of the absorbance readings that the standard curve covers should be as large as possible, with the minimum accepted range to be 0.5. As magnitude of the standard curve slope increase, the accuracy of the assay would in turn increase. After numerous combinations were tested, it was concluded that the parameter of 40ng Osteocalcin coated, 50 $\mu$ L of 240 $\mu$ g/mL scFv coincubated with 50 $\mu$ L samples and 100 $\mu$ L of 1:2500 anti-myc detection antibody was optimal. Figure 4.16 showed the generated standard curve from the competitive ELISA using the mentioned parameter.

The next step of evaluating the developed Osteocalcin competitive assay was to compare the result with an existing commercial Osteocalcin ELISA kit. To carry this comparison, OVX and Sham rat serum samples at 4 weeks and 12 weeks were used for analysis, and the ratios of serum Osteocalcin of the 12 weeks samples to 4 weeks sample were plotted. Figure 4.17 showed that both ELISA's yielded similar trends despite the ratios being different. It is also very apparent that the variation of the assay using the anti-Osteocalcin scFv was much greater

than the commercial kit purchased from IDS. There are several factors that may lead to such variations. First, the two assays were done at two different times. Commercial ELISA kit analyzed serum samples that were stored for 4 months, while the scFv ELISA analyzed the same samples that were stored for over 16 months. During the time of storage and repeated freeze-thaw of samples, some proteins might have undergone degradation, greatly increasing the variation (42). Another factor could be due to the increase in serum sample volume during co-incubation step. While using commercial ELISA kit, 100 $\mu$ L of primary antibody and 20 $\mu$ L of serum sample was used for incubation. However, 50 $\mu$ L of primary antibody and 50 $\mu$ L of serum sample was used for the scFv method in order to maximize detection and minimize antibody used. The increase ratio of serum sample to primary antibody solution may increase the viscosity of the incubation solution and increase the difficulty for scFv to scavenge the marker. Although further optimization with biological samples are needed, the result obtained showed evidence that scFv potentially can become an alternative to conventional IgG antibody.

### **5.5. Phage Display of CTX-binding scFv**

Our last target antigen for developing scFv against was the early bone turnover marker CTX. It is a characteristic cross-linked polypeptide that is generated during bone resorption. As shown in Figure 4.18, the panning efficiency of the first phage screening attempt was consistent with the screen against RANK. After DNA sequencing analysis, however, it was revealed that all

10 clones picked possessed identical DNA sequence. Moreover, this clone contained an amber codon within one of the random sites on the heavy chain, which was a major obstacle in expressing scFv. As mentioned earlier, phage display utilizes two *E.coli* strains – TG1 and HB2151. TG1 is used primarily for phage screening because it is an amber suppressing strain, so that all amber codons would be translated as glutamine during protein translation. Since the pIT2 is a phage display plasmid construct which separates the scFv DNA and the M13 pIII protein with an amber codon, such a genotype is useful because it allows the synthesis of scFv-pIII fusion for packaging scFv-displaying phage. On the other hand, HB2151 is good for expression but a non-amber suppressing strain. Once a phage has successfully infected HB2151 and incorporated its phagemid within the cell, HB2151 can be induced for expression. However, since HB2151 will terminate translation at the amber codon, only free soluble scFv is expressed. Such system works well together with one major limitation – If an amber codon exists within any of the random sites, these sites will be expressed as glutamine during phage screening stage. However, if such phage is to infect HB2151 for expression, it will lead to premature translation termination. This problem is a rare one but it is what we were facing with our single positive clone. In trying to avoid this obstacle, other positive clones were picked for DNA sequencing to try and identify at least one that would not contain an amber codon within the scFv DNA sequence. However, over 30 clones were sequenced but all possessed the identical, amber-containing sequence. Subsequently, 2 more phage screening attempts were committed using fresh phage library aliquots in trying to screen for

a different CTX-binding scFv-phage clone. During the later 2 attempts, over 20 clones were sequenced and all positive clones were found to possess identical sequence as the one first identified.

Although unfortunate, this result was not entirely a surprise to us. While the previous two antigens used for screening were over 45 amino acids long, the CTX antigen used for this screening contained only 8 amino acids. Phage display is an *in vitro* technique that mimics antibody affinity maturation within a biological immune system such as mice. Therefore, as antigen becomes larger, the number of epitope sites also increases. In the case of CTX during this panning process, we suspected even before the screening that very few CTX-binding clones would be identified due to the size of the antigen used. The result generated after 3 screening attempts further confirmed our prediction.

Even though HB2151 could not be used for expressing the scFv, site directed mutagenesis was an alternative where the amber codon separating the scFv and pIII DNA could be mutated to a TAA stop codon instead. This method allows expression of soluble phage-free scFv using TG1 but comes at the cost of expression efficiency as TG1 is known to be not as efficient as HB2151 in protein expression. Although such method can be done, we decided not to pursue this route. The reason is that the Tomlinson I library was also used by Saikiran Sharma from Dr. Suresh's lab in trying to generate scFv for binding various antigens. Interestingly, the CTX-binding phage clone identified in this phage screening process was also identified in 2 other phage screening that Saikiran has performed. As a result, we believed that even if site-directed mutagenesis was

performed and soluble scFv was expressed, such scFv can be a non-specific binder, yielding inaccurate result and false conclusion in future studies.

Few thoughts were given into amplifying the Tomlinson J library to try to look for CTX-binding scFv from the library. This idea, however, was quickly dismissed due to two main reasons. First, because CTX contains only 8 amino acids, the probability of screening a different scFv clone from 3 separate screenings using the Tomlinson I library would be very low. Moreover, the Tomlinson J library is not a fully randomized library – Although both libraries contain randomized amino acid at the same site, the randomized codon for the Tomlinson J library has the “NNK” format. This means that the last codon of all randomized amino acid is keto nucleotide, which corresponds to either G or T. Such characteristic further increases the probability that a pre-mature amber (TAG) codon would be present at the random sites.

Although we have failed to develop a CTX-binding scFv, much was learned about the limitation of phage display in general. While phage display is an effective way to screen for scFv targeting medium to large antigens, it becomes problematic for very small antigens. These antigens are either too small to present a unique epitope for binding or they are simply inaccessible for the scFv-phage to bind. Both of these possibilities would result in little or no positive binders or, in our case, non-specific binders.

## 6. Conclusion

To summarize our findings, we believed that phage display is an effective technique to substitute the *in vivo* method of antibody generation by animal immunization. Although with lower binding affinity, scFv's identified and expressed from phage display library were much cheaper and took much less time to develop and were much easier to handle due to their smaller sizes. Given the antigens were at an appropriate size (>2kDa), scFv with specific binding affinity can be identified and expressed within one month from a large library.

With the successful attempt at generating both RANK-binding and Osteocalcin-binding scFv's, along with previously done studies by various research group, it is evident that the phage display technique can be used for generating scFv against virtually an infinite number of antigens (61, 110). With the anti-RANK scFv ELISA result, it shows that scFv, although not as effective as conventional hybridoma IgG antibody, has the potential in becoming a drug targeting vehicle and should merit further *in vivo* investigation.

Although the immunoassay developed showed a large degree of variation in comparison with the commercially available kit, the similar trend obtained in the study showed that scFv in fact has the potential to function similarly as conventional antibody in the diagnostic field.

While this project was mostly geared towards the treatment and diagnostic of osteoporosis, the application of this study is useful but not limit to osteoporosis only. With various reports in the literature suggesting the importance of osteoclast activity, the relative success and potential of bisphosphonates in osteoarthritis, the

development of RANK-targeting therapeutics and bisphosphonate-responsive diagnostic assay can also be cross applied to bone modifying disease such as osteoarthritis or any other diseases that are responsive to bisphosphonate and cause by increased osteoclast activity.

## 7. Future Directions

With 2 scFv's having binding affinity to 2 different kinds of antigens, we have opened up opportunity to explore both the therapeutics and diagnostics aspect for osteoporosis and other bone modifying disease such as osteoarthritis. In the near future, our lab will be focusing mostly on anti-RANK scFv and the therapeutics aspect. The anti-RANK scFv has now been given to lab colleague Madhuri Newa for chemical conjugation to calcitonin and to conduct ongoing cell-based and upcoming in vivo pharmacokinetics studies.

Since we have failed to meet our initial expectations of generating at least 3 scFv's for each antigen, it would be beneficial to incorporate the Tomlinson J library in subsequent screening for other antigens in attempting to isolate more antigen-binding scFv's.

Due to the inherent lack of structural stability of scFv, our long term goal is to identify strategies to prolong scFv's systemic and storage half-life. Since scFv (~30kDa) is much smaller than conventional IgG antibody (~150kDa) and only contain amino acids crucial for binding, common antibody stabilization strategy such as PEGylation (71, 111-113) should be used with caution because conjugation to any amino acid residue can greatly affect the structural confirmation and the scFv binding affinity. Methods such as non-natural amino acid substitution and  $\beta$ -amino acid substitution are notable substitute strategies to increase scFv stability against proteolytic degradation (72, 114-117). However, even though scFv is considered to be a small when compare to IgG, it is still a

fairly large protein, which makes peptidomimetics a feasible but challenging method. In addition, improper refolding after modifications may also occur.

In realizing the limitations of phage display against small antigens in the phage selection against CTX, few reports have described strategies to overcome this issue (118). Prior to panning, the small antigen is first chemically conjugated to an anchor protein to increase the size to make the antigen more accessible to scFv phages. During the phage selection step, the scFv phages are then co-incubated with the pure anchor protein to remove any anchor protein-binding scFv, ensuring the bound scFv isolated selectively binds to the antigen of interest. This method can be used in the future in trying to solve the problem observed in the CTX-screening. If proven successful, the same procedure can be applied to isolate another small bone-turnover marker, NTX, to generate a panel of bone-turnover marker-specific scFv's. This potential panel can be used to develop either an immunodiagnostic assay or an all-in-one point-of-care test kit, which would give physicians and pharmacists tremendous accuracy in evaluating disease progression or treatment effectiveness in patients.

## 8. Bibliography

1. Osteoporosis at-a-glance [Internet].; 2011. Available from: [www.osteoporosis.ca](http://www.osteoporosis.ca).
2. Sambrook P, Cooper C. Osteoporosis. *Lancet*. 2006;367(9527):2010-8.
3. Kanis JA. Osteoporosis III: Diagnosis of osteoporosis and assessment of fracture risk. *Lancet*. 2002;359(9321):1929-36.
4. Manolagas SC. Birth and death of bone cells: Basic regulatory mechanisms and implications for the pathogenesis and treatment of osteoporosis. *Endocr Rev*. 2000;21(2):115-37.
5. Dempster DW, Lindsay R. Pathogenesis of osteoporosis. *Lancet*. 1993;341(8848):797-801.
6. Raisz LG. Pathogenesis of osteoporosis: Concepts, conflicts, and prospects. *J Clin Invest*. 2005;115(12):3318-25.
7. Teitelbaum SL, Ross FP. Genetic regulation of osteoclast development and function. *Nature Reviews Genetics*. 2003;4(8):638-49.
8. Rodan GA, Martin TJ. Therapeutic approaches to bone diseases. *Science*. 2000;289(5484):1508-14.
9. Mödder UIL, Riggs BL, Spelsberg TC, Fraser DG, Atkinson EJ, Arnold R, et al. Dose-response of estrogen on bone versus the uterus in ovariectomized mice. *European Journal of Endocrinology*. 2004;151(4):503-10.
10. Kameda T, Mano H, Yuasa T, Mori Y, Miyazawa K, Shiokawa M, et al. Estrogen inhibits bone resorption by directly inducing apoptosis of the bone-resorbing osteoclasts. *J Exp Med*. 1997;186(4):489-95.
11. Teitelbaum SL. Bone resorption by osteoclasts. *Science*. 2000;289(5484):1504-8.
12. Suda T, Takahashi N, Udagawa N, Jimi E, Gillespie MT, Martin TJ. Modulation of osteoclast differentiation and function by the new members of the tumor necrosis factor receptor and ligand families. *Endocr Rev*. 1999;20(3):345-57.
13. Takayanagi H. Mechanistic insight into osteoclast differentiation in osteoimmunology. *Journal of Molecular Medicine*. 2005;83(3):170-9.
14. Hofbauer LC, Heufelder AE. Role of receptor activator of nuclear factor- $\kappa$ B ligand and osteoprotegerin in bone cell biology. *Journal of Molecular Medicine*. 2001;79(5-6):243-53.

15. Burgess TL, Qian Y-, Kaufman S, Ring BD, Van G, Capparelli C, et al. The ligand for osteoprotegerin (OPGL) directly activates mature osteoclasts. *J Cell Biol.* 1999;145(3):527-38.
16. Khosla S. Minireview: The OPG/RANKL/RANK system. *Endocrinology.* 2001;142(12):5050-5.
17. Boyle WJ, Simonet WS, Lacey DL. Osteoclast differentiation and activation. *Nature.* 2003;423(6937):337-42.
18. Filvaroff E, Derynck R. Bone remodelling: A signalling system for osteoclast regulation. *Current Biology.* 1998 9/24;8(19):R679-82.
19. Bucay N, Sarosi I, Dunstan CR, Morony S, Tarpley J, Capparelli C, et al. Osteoprotegerin-deficient mice develop early onset osteoporosis and arterial calcification. *Genes and Development.* 1998;12(9):1260-8.
20. Eghbali-Fatourehchi G, Khosla S, Sanyal A, Boyle WJ, Lacey DL, Riggs BL. Role of RANK ligand in mediating increased bone resorption in early postmenopausal women. *J Clin Invest.* 2003;111(8):1221-30.
21. Yasuda H, Shima N, Nakagawa N, Mochizuki S-, Yano K, Fujise N, et al. Identity of osteoclastogenesis inhibitory factor (OCIF) and osteoprotegerin (OPG): A mechanism by which OPG/OCIF inhibits osteoclastogenesis in vitro. *Endocrinology.* 1998;139(3):1329-37.
22. Simonet WS, Lacey DL, Dunstan CR, Kelley M, Chang M-, Lüthy R, et al. Osteoprotegerin: A novel secreted protein involved in the regulation of bone density. *Cell.* 1997;89(2):309-19.
23. Wang Y, Grainger DW. siRNA knock-down of RANK signaling to control osteoclast-mediated bone resorption. *Pharm Res.* 2010:1-12.
24. Zhang S, Liu C, Huang P, Zhou S, Ren J, Kitamura Y, et al. The affinity of human RANK binding to its ligand RANKL. *Arch Biochem Biophys.* 2009 7/1;487(1):49-53.
25. Takayanagi H, Kim S, Matsuo K, Suzuki H, Suzuki T, Sato K, et al. RANKL maintains bone homeostasis through c-fos-dependent induction of interferon- $\beta$ . *Nature.* 2002;416(6882):744-9.
26. Kanazawa K, Kudo A. Self-assembled RANK induces osteoclastogenesis ligand-independently. *Journal of Bone and Mineral Research.* 2005;20(11):2053-60.
27. Iwamoto K, Miyamoto T, Sawatani Y, Hosogane N, Hamaguchi I, Takami M, et al. Dimer formation of receptor activator of nuclear factor  $\kappa$ B induces incomplete osteoclast formation. *Biochem Biophys Res Commun.* 2004 12/3;325(1):229-34.
28. Riggs BL, Melton III LJ. The prevention and treatment of osteoporosis. *N Engl J Med.* 1992;327(9):620-7.

29. Ettinger B, San Martin J, Crans G, Pavo I. Differential effects of teriparatide on BMD after treatment with raloxifene or alendronate. *Journal of Bone and Mineral Research*. 2004;19(5):745-51.
30. Delmas PD. Treatment of postmenopausal osteoporosis. *Lancet*. 2002;359(9322):2018-26.
31. Iida S, Kakudo S, Mori Y, Matsui M, Magota K, Kitajima Y, et al. Human calcitonin has the same inhibitory effect on osteoclastic bone resorption by human giant cell tumor cells as salmon calcitonin. *Calcif Tissue Int*. 1996;59(2):100-4.
32. Rogers MJ, Gordon S, Benford HL, Coxon FP, Luckman SP, Monkkonen J, et al. Cellular and molecular mechanisms of action of bisphosphonates. *Cancer*. 2000;88(12 SUPPL.):2961-78.
33. Fisher JE, Rogers MJ, Halasy JM, Luckman SP, Hughes DE, Masarachia PJ, et al. Alendronate mechanism of action: Geranylgeraniol, an intermediate in the mevalonate pathway, prevents inhibition of osteoclast formation, bone resorption, and kinase activation in vitro. *Proc Natl Acad Sci U S A*. 1999;96(1):133-8.
34. Storm T, Thamsborg G, Steiniche T, Genant HK, Sorensen OH. Effect of intermittent cyclical etidronate therapy on bone mass and fracture rate in women postmenopausal osteoporosis. *N Engl J Med*. 1990;322(18):1265-71.
35. Watts NB, Harris ST, Genant HK, Wasnich RD, Miller PD, Jackson RD, et al. Intermittent cyclical etidronate treatment of postmenopausal osteoporosis. *N Engl J Med*. 1990;323(2):73-9.
36. McClung MR, Michael Lewiecki E, Cohen SB, Bolognese MA, Woodson GC, Moffett AH, et al. Denosumab in postmenopausal women with low bone mineral density. *N Engl J Med*. 2006;354(8):821-31.
37. Miller PD, Bolognese MA, Lewiecki EM, McClung MR, Ding B, Austin M, et al. Effect of denosumab on bone density and turnover in postmenopausal women with low bone mass after long-term continued, discontinued, and restarting of therapy: A randomized blinded phase 2 clinical trial. *Bone*. 2008;43(2):222-9.
38. Burkiewicz JS, Scarpace SL, Bruce SP. Denosumab in osteoporosis and oncology. *Ann Pharmacother*. 2009;43(9):1445-55.
39. Cummings SR, Martin JS, McClung MR, Siris ES, Eastell R, Reid IR, et al. Denosumab for prevention of fractures in postmenopausal women with osteoporosis. *N Engl J Med*. 2009;361(8):756-65.
40. Yasuda Y, Kaleta J, Brömme D. The role of cathepsins in osteoporosis and arthritis: Rationale for the design of new therapeutics. *Adv Drug Deliv Rev*. 2005;57(7):973-93.
41. Bikle DD. Biochemical markers in the assessment of bone disease. *Am J Med*. 1997;103(5):427-36.

42. Civitelli R, Armamento-Villareal R, Napoli N. Bone turnover markers: Understanding their value in clinical trials and clinical practice. *Osteoporosis Int.* 2009;20(6):843-51.
43. Cremers S, Garnero P. Biochemical markers of bone turnover in the clinical development of drugs for osteoporosis and metastatic bone disease: Potential uses and pitfalls. *Drugs.* 2006;66(16):2031-58.
44. Delmas PD. Biochemical markers of bone turnover for the clinical assessment of metabolic bone disease. *Endocrinol Metab Clin North Am.* 1990;19(1):1-18.
45. Delmas PD, Eastell R, Garnero P, Seibel MJ, Stepan J. The use of biochemical markers of bone turnover in osteoporosis. *Osteoporosis Int.* 2000;11(SUPPL. 6):S2-S17.
46. Eastell R, Hannon RA. Biomarkers of bone health and osteoporosis risk. *Proc Nutr Soc.* 2008;67(2):157-62.
47. Garnero P, Delmas PD. Biochemical markers of bone turnover: Applications for osteoporosis. *Endocrinol Metab Clin North Am.* 1998;27(2):303-23.
48. Indumati V, Patil VS. Biochemical markers of bone remodeling in osteoporosis - current concepts. *Journal of Clinical and Diagnostic Research.* 2010;4(1):2089-97.
49. Szulc P, Delmas PD. Biochemical markers of bone turnover: Potential use in the investigation and management of postmenopausal osteoporosis. *Osteoporosis Int.* 2008;19(12):1683-704.
50. McCormick RK. Osteoporosis: Integrating biomarkers and other diagnostic correlates into the management of bone fragility. *Alternative Medicine Review.* 2007;12(2):113-45.
51. Epstein S. Serum and urinary markers of bone remodeling: Assessment of bone turnover. *Endocr Rev.* 1988;9(4):437-49.
52. Reginster J-, Collette J, Neuprez A, Zegels B, Deroisy R, Bruyere O. Role of biochemical markers of bone turnover as prognostic indicator of successful osteoporosis therapy. *Bone.* 2008;42(5):832-6.
53. Brown JP, Albert C, Nassar BA, Adachi JD, Cole D, Davison KS, et al. Bone turnover markers in the management of postmenopausal osteoporosis. *Clin Biochem.* 2009;42(10-11):929-42.
54. Delmas PD. Clinical use of biochemical markers of bone remodeling in osteoporosis. *Bone.* 1992;13(1 SUPPL.):S17-21.
55. Lewiecki EM. Benefits and limitations of bone mineral density and bone turnover markers to monitor patients treated for osteoporosis. *Current Osteoporosis Reports.* 2010;8(1):15-22.

56. Schneider DL, Barrett-Connor EL. Urinary N-telopeptide levels discriminate normal, osteopenic, and osteoporotic bone mineral density. *Arch Intern Med.* 1997;157(11):1241-5.
57. Pozzi S, Vallet S, Mukherjee S, Cirstea D, Vaghela N, Santo L, et al. High-dose zoledronic acid impacts bone remodeling with effects on osteoblastic lineage and bone mechanical properties. *Clinical Cancer Research.* 2009;15(18):5829-39.
58. Rissanen JP, Suominen MI, Peng Z, Halleen JM. Secreted tartrate-resistant acid phosphatase 5b is a marker of osteoclast number in human osteoclast cultures and the rat ovariectomy model. *Calcif Tissue Int.* 2008;82(2):108-15.
59. Stockwin LH, Holmes S. Antibodies as therapeutic agents: Vive la renaissance! *Expert Opinion on Biological Therapy.* 2003;3(7):1133-52.
60. Presta LG. Molecular engineering and design of therapeutic antibodies. *Curr Opin Immunol.* 2008;20(4):460-70.
61. Weisser NE, Hall JC. Applications of single-chain variable fragment antibodies in therapeutics and diagnostics. *Biotechnol Adv.* 2009;27(4):502-20.
62. Nicolaidis NC, Sass PM, Grasso L. Monoclonal antibodies: A morphing landscape for therapeutics. *Drug Dev Res.* 2006;67(10):781-9.
63. Kohler G, Milstein C. Continuous cultures of fused cells secreting antibody of predefined specificity. *Nature.* 1975;256(5517):495-7.
64. Smolen JS, Steiner G. Therapeutic strategies for rheumatoid arthritis. *Nature Reviews Drug Discovery.* 2003;2(6):473-88.
65. Rankin ECC, Choy EHS, Kassimos D, Kingsley GH, Sopwith AM, Isenberg DA, et al. The therapeutic effects of an engineered human anti-tumour necrosis factor alpha antibody (CDP571) in rheumatoid arthritis. *Br J Rheumatol.* 1995;34(4):334-42.
66. Agus DB, Gordon MS, Taylor C, Natale RB, Karlan B, Mendelson DS, et al. Phase I clinical study of pertuzumab, a novel HER dimerization inhibitor, in patients with advanced cancer. *Journal of Clinical Oncology.* 2005;23(11):2534-43.
67. Goldenberg DM. Monoclonal antibodies in cancer detection and therapy. *Am J Med.* 1993;94(3):297-312.
68. Schrama D, Reisfeld RA, Becker JC. Antibody targeted drugs as cancer therapeutics. *Nature Reviews Drug Discovery.* 2006;5(2):147-59.
69. Wu AM, Olafsen T. Antibodies for molecular imaging of cancer. *Cancer Journal.* 2008;14(3):191-7.

70. Hughes C, Faurholm B, Dell'Accio F, Manzo A, Seed M, Eltawil N, et al. Human single-chain variable fragment that specifically targets arthritic cartilage. *Arthritis Rheum.* 2010;62(4):1007-16.
71. Chapman AP. PEGylated antibodies and antibody fragments for improved therapy: A review. *Adv Drug Deliv Rev.* 2002;54(4):531-45.
72. Gante J. Peptidomimetics - tailored enzyme inhibitors. *Angewandte Chemie - International Edition in English.* 1994;33(17):1699-720.
73. Smith GP. Filamentous fusion phage: Novel expression vectors that display cloned antigens on the virion surface. *Science.* 1985;228(4705):1315-7.
74. Azzazy HME, Highsmith Jr WE. Phage display technology: Clinical applications and recent innovations. *Clin Biochem.* 2002;35(6):425-45.
75. Burritt JB, Bond CW, Doss KW, Jesaitis AJ. Filamentous phage display of oligopeptide libraries. *Anal Biochem.* 1996;238(1):1-13.
76. Dunn IS. Phage display of proteins. *Curr Opin Biotechnol.* 1996;7(5):547-53.
77. Koivunen E, Gay DA, Ruoslahti E. Selection of peptides binding to the  $\alpha 5\beta 1$  integrin from phage display library. *J Biol Chem.* 1993;268(27):20205-10.
78. Lowman HB. Selecting high-affinity binding proteins by monovalent phage display. *Biochemistry (N Y).* 1991;30(45):10832-8.
79. Parmley SF, Smith GP. Filamentous fusion phage cloning vectors for the study of epitopes and design of vaccines. *Adv Exp Med Biol.* 1989;251:215-8.
80. Pereira S, Maruyama H, Siegel D, Van Belle P, Elder D, Curtis P, et al. A model system for detection and isolation of a tumor cell surface antigen using antibody phage display. *J Immunol Methods.* 1997;203(1):11-24.
81. Scott JK, Smith GP. Searching for peptide ligands with an epitope library. *Science.* 1990;249(4967):386-90.
82. Spear MA, Breakefield XO, Beltzer J, Schuback D, Weissleder R, Pardo FS, et al. Isolation, characterization, and recovery of small peptide phage display epitopes selected against viable malignant glioma cells. *Cancer Gene Ther.* 2001;8(7):506-11.
83. Winter G, Griffiths AD, Hawkins RE, Hoogenboom HR. Making antibodies by phage display technology. *Annu Rev Immunol.* 1994;12:433-55.
84. Kehoe JW, Kay BK. Filamentous phage display in the new millennium. *Chem Rev.* 2005;105(11):4056-72.
85. Pini A, Bracci L. Phage display of antibody fragments. *Current Protein and Peptide Science.* 2000;1(2):155-69.

86. Rondot S, Koch J, Breitling F, Dübel S. A helper phage to improve single-chain antibody presentation in phage display. *Nat Biotechnol.* 2001;19(1):75-8.
87. Barbas III CF, Kang AS, Lerner RA, Benkovic SJ. Assembly of combinatorial antibody libraries on phage surfaces: The gene III site. *Proc Natl Acad Sci U S A.* 1991;88(18):7978-82.
88. Petrenko VA, Smith GP. Phages from landscape libraries as substitute antibodies. *Protein Eng.* 2000;13(8):589-92.
89. Jespers LS, Messens JH, De Keyser A, Eeckhout D, Van den Brande I, Gansemans YG, et al. Surface expression and ligand-based selection of cDNAs fused to filamentous phage gene VI. *Bio/Technology.* 1995;13(4):378-82.
90. Kishchenko G, Batliwala H, Makowski L. Structure of a foreign peptide displayed on the surface of bacteriophage M13. *J Mol Biol.* 1994;241(2):208-13.
91. Griffiths AD, Malmqvist M, Marks JD, Bye JM, Embleton MJ, McCafferty J, et al. Human anti-self antibodies with high specificity from phage display libraries. *EMBO J.* 1993;12(2):725-34.
92. Nissim A, Hoogenboom HR, Tomlinson IM, Flynn G, Midgley C, Lane D, et al. Antibody fragments from a 'single pot' phage display library as immunochemical reagents. *EMBO J.* 1994;13(3):692-8.
93. Rader C, Barbas III CF. Phage display of combinatorial antibody libraries. *Curr Opin Biotechnol.* 1997;8(4):503-8.
94. Hoogenboom HR, Griffiths AD, Johnson KS, Chiswell DJ, Hudson P, Winter G. Multi-subunit proteins on the surface of filamentous phage: Methodologies for displaying antibody (fab) heavy and light chains. *Nucleic Acids Res.* 1991;19(15):4133-7.
95. Matthews DJ, Wells JA. Substrate phage: Selection of protease substrates by monovalent phage display. *Science.* 1993;260(5111):1113-7.
96. Hoogenboom HR, De Brune AP, Hufton SE, Hoet RM, Arends J-, Roovers RC. Antibody phage display technology and its applications. *Immunotechnology.* 1998;4(1):1-20.
97. Griffiths AD, Williams SC, Hartley O, Tomlinson IM, Waterhouse P, Crosby WL, et al. Isolation of high affinity human antibodies directly from large synthetic repertoires. *EMBO J.* 1994;13(14):3245-60.
98. Hawkins RE, Russell SJ, Winter G. Selection of phage antibodies by binding affinity. mimicking affinity maturation. *J Mol Biol.* 1992;226(3):889-96.
99. Lowman HB, Wells JA. Affinity maturation of human growth hormone by monovalent phage display. *J Mol Biol.* 1993;234(3):564-478.

100. Poul M-, Marks JD. Targeted gene delivery to mammalian cells by filamentous bacteriophage. *J Mol Biol.* 1999;288(2):203-11.
101. Tian F, Tsao M-, Schultz PG. A phage display system with unnatural amino acids. *J Am Chem Soc.* 2004;126(49):15962-3.
102. Manicourt D-, Devogelaer J-, Azria M, Silverman S. Rationale for the potential use of calcitonin in osteoarthritis. *Journal of Musculoskeletal Neuronal Interactions.* 2005;5(3):285-93.
103. Bingham III CO, Buckland-Wright JC, Garnero P, Cohen SB, Dougados M, Adami S, et al. Risedronate decreases biochemical markers of cartilage degradation but does not decrease symptoms or slow radiographic progression in patients with medial compartment osteoarthritis of the knee: Results of the two-year multinational knee osteoarthritis structural arthritis study. *Arthritis Rheum.* 2006;54(11):3494-507.
104. Devogelaer J-. Treatment of bone diseases with bisphosphonates, excluding osteoporosis. *Curr Opin Rheumatol.* 2000;12(4):331-5.
105. Bezerra MC, Carvalho JF, Prokopowitsch AS, Pereira RMR. RANK, RANKL and osteoprotegerin in arthritic bone loss. *Brazilian Journal of Medical and Biological Research.* 2005;38(2):161-70.
106. Crotti TN, Smith MD, Weedon H, Ahern MJ, Findlay DM, Kraan M, et al. Receptor activator NF- $\kappa$ B ligand (RANKL) expression in synovial tissue from patients with rheumatoid arthritis, spondyloarthropathy, osteoarthritis, and from normal patients: Semiquantitative and quantitative analysis. *Ann Rheum Dis.* 2002;61(12):1047-54.
107. Tat SK, Pelletier J-, Velasco CR, Padrines M, Martel-Pelletier J. New perspective in osteoarthritis: The OPG and RANKL system as a potential therapeutic target? *Keio J Med.* 2009;58(1):29-40.
108. Karsdal MA, Leeming DJ, Dam EB, Henriksen K, Alexandersen P, Pastoureau P, et al. Should subchondral bone turnover be targeted when treating osteoarthritis? *Osteoarthritis Cartilage.* 2008;16(6):638-46.
109. Kwan Tat S, Lajeunesse D, Pelletier J-, Martel-Pelletier J. Targeting subchondral bone for treating osteoarthritis: What is the evidence? *Best Pract Res Clin Rheumatol.* 2010;24(1):51-70.
110. Yokota T, Milenic DE, Whitlow M, Schlom J. Rapid tumor penetration of a single-chain fv and comparison with other immunoglobulin forms. *Cancer Res.* 1992;52(12):3402-8.
111. Caliceti P, Veronese FM. Pharmacokinetic and biodistribution properties of poly(ethylene glycol)-protein conjugates. *Adv Drug Deliv Rev.* 2003 9/26;55(10):1261-77.

112. Milton Harris J, Chess RB. Effect of pegylation on pharmaceuticals. *Nature Reviews Drug Discovery*. 2003;2(3):214-21.
113. Pasut G, Guiotto A, Veronese FM. Protein, peptide and non-peptide drug PEGylation for therapeutic application. *Expert Opin Ther Patents*. 2004 06/01; 2011/03;14(6):859-94.
114. Godballe T, Nilsson LL, Petersen PD, Jenssen H. Antimicrobial  $\beta$ -peptides and  $\alpha$ -peptoids. *Chemical Biology and Drug Design*. 2011;77(2):107-16.
115. Pauletti GM, Gangwar S, Siahaan TJ, Aubé J, Borchardt RT. Improvement of oral peptide bioavailability: Peptidomimetics and prodrug strategies. *Adv Drug Deliv Rev*. 1997;27(2-3):235-56.
116. Veronese FM, Morpurgo M. Bioconjugation in pharmaceutical chemistry. *Farmaco*. 1999;54(8):497-516.
117. Werle M, Bernkop-Schnürch A. Strategies to improve plasma half life time of peptide and protein drugs. *Amino Acids*. 2006;30(4):351-67.
118. Barderas R, Shochat S, Martínez-Torrecuadrada J, Altschuh D, Meloen R, Ignacio Casal J. A fast mutagenesis procedure to recover soluble and functional scFvs containing amber stop codons from synthetic and semisynthetic antibody libraries. *J Immunol Methods*. 2006;312(1-2):182-9.